10962-E250

PACIFIC GEOPHYSICAL LTD.
REPORT ON THE
CONTROLLED SOURCE AUDIO
MAGNETOTELLURIC SURVEY (CSAMT)
ON THE
BAR PROPERTY
FORT STEELE MINING DIVISION
BRITISH COLUMBIA

16697

PACIFIC GEOPHYSICAL LTD.

REPORT

ON THE

CONTROLLED SOURCE AUDIO MAGNETOTELLURIC SURVEY (CSAMT)

ON THE

BAR PROPERTY

FORT STEELE MINING DIVISION

BRITISH COLUMBIA

LATITUDE: 49°28' N LONGITUDE: 115°55'W

N.T.S. 82G5/W

CLAIMS: VINE 55, BAR1, BAR 6 - 18, BELLEVILLE CR. GRANT, LOCKOUT CR. GRANT

OWNER: JOHN M. LEASK
OPERATOR: JOHN M. LEASK

BY

PAUL A. CARTWRIGHT, P. Geoph.
GEOPHYSICIST

DATED: January 15, 1988

TABLE OF CONTENTS

PAGE

PART A REPORT

PART B ILLUSTRATION

PART C

PART A REPORT

1) INTRODUCTION

A Controlled Source Audio Magnetotelluric (CSAMT) survey has been completed on the Bar Property on behalf of John M. Leask in Fort Steele Mining Division, British Columbia.

The property is located approximately 13 km southwest of Cranbrook, B.C. Access is by wheeled vehicle over a system of logging roads leading east from the Crowsnest Highway at Lumberton, B.C.

The CSAMT technique is a relatively new method used to map the resistivity configuration of the earth. Part C of this report describes the method in some detail and also provides some case histories.

The objective of the CSAMT survey was to evaluate the property for zones of low resistivity which could be indicative of the presence of conductive sulphide mineralization similar to the lead-zinc ore of the Sullivan Mine located 30 km north at Kimberley, B.C.

A Phoenix Model V-3 CSAMT receiver unit was used to make the geophysical measurements in conjunction with a Phoenix IPT-1/AC3004 transmitter powered by a 3 kw motor generator. A copper wire approximately 4 km in length and grounded at both ends was used as the transmitter dipole, as illustrated on Figure 3, a 1:50,000 location map showing the survey lines and the transmitter wire.

Six electric field measurements and one magnetic field measurement were made simultaneously at each setup. The electric field measurements used an interelectrode spacing of 200 meters along the survey lines, while a horizontal magnetic measurement was made perpendicular to the line at 1200 meter intervals. Data was recorded at 15 frequencies ranging in binary steps from 4096 Hz to 0.25 Hz.

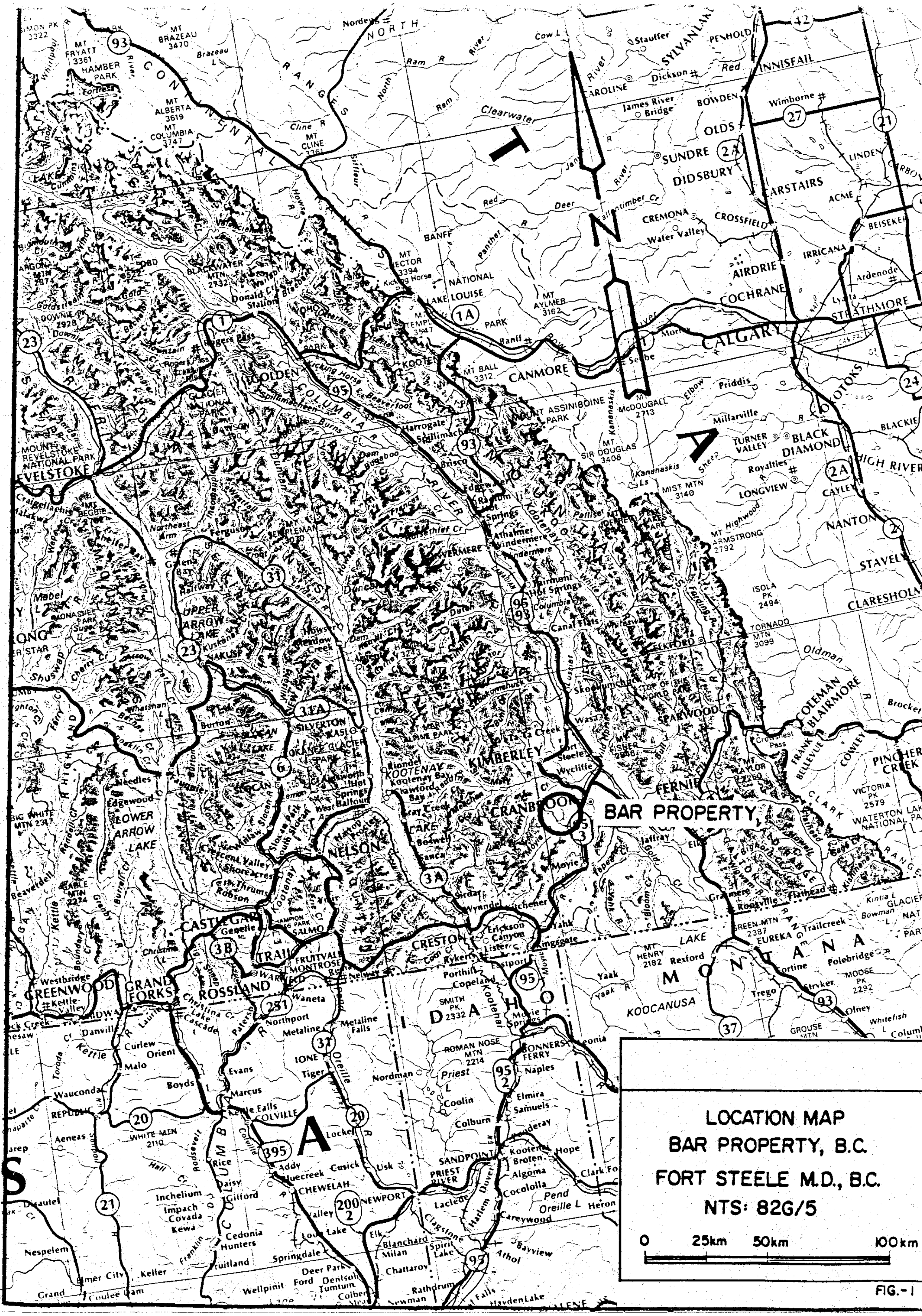

LOCATION MAP
BAR PROPERTY, B.C.
FORT STEELE M.D., B.C.
NTS: 82G/5

FIG.-1

Field work took place during late September and early October, 1987 under the supervision of Paul A. Cartwright, P. Geoph., whose certificate of qualification is included in this report.

2) CLAIM INFORMATION

The Bar Claim Group consists of 15 contiguous claims totalling 106 units as well as 2 Crown Grants.

CLAIM NAME	UNITS	RECORD NO.	RECORD DATE
Vine 55	18	1871	July 18, 1983
Bar 1	20	2015	November 10, 1983
Bar 6	16	2028	December 14, 1983
Bar 7	6	2029	December 14, 1983
Bar 8	1	2164	July 3, 1984
Bar 9	1	2165	July 3, 1984
Bar 10	1	2166	July 3, 1984
Bar 11	1	2167	July 3, 1984
Bar 12	18	2168	July 3, 1984
Bar 13	10	2169	July 3, 1984
Bar 14	1	2170	July 3, 1984
Bar 15	1	2171	July 3, 1984
Bar 16	1	2172	July 3, 1984
Bar 17	6	2354	February 20, 1985
Bar 18	3	2355	February 20, 1985
Belleville	Crown Grant		
Lookout	Crown Grant		

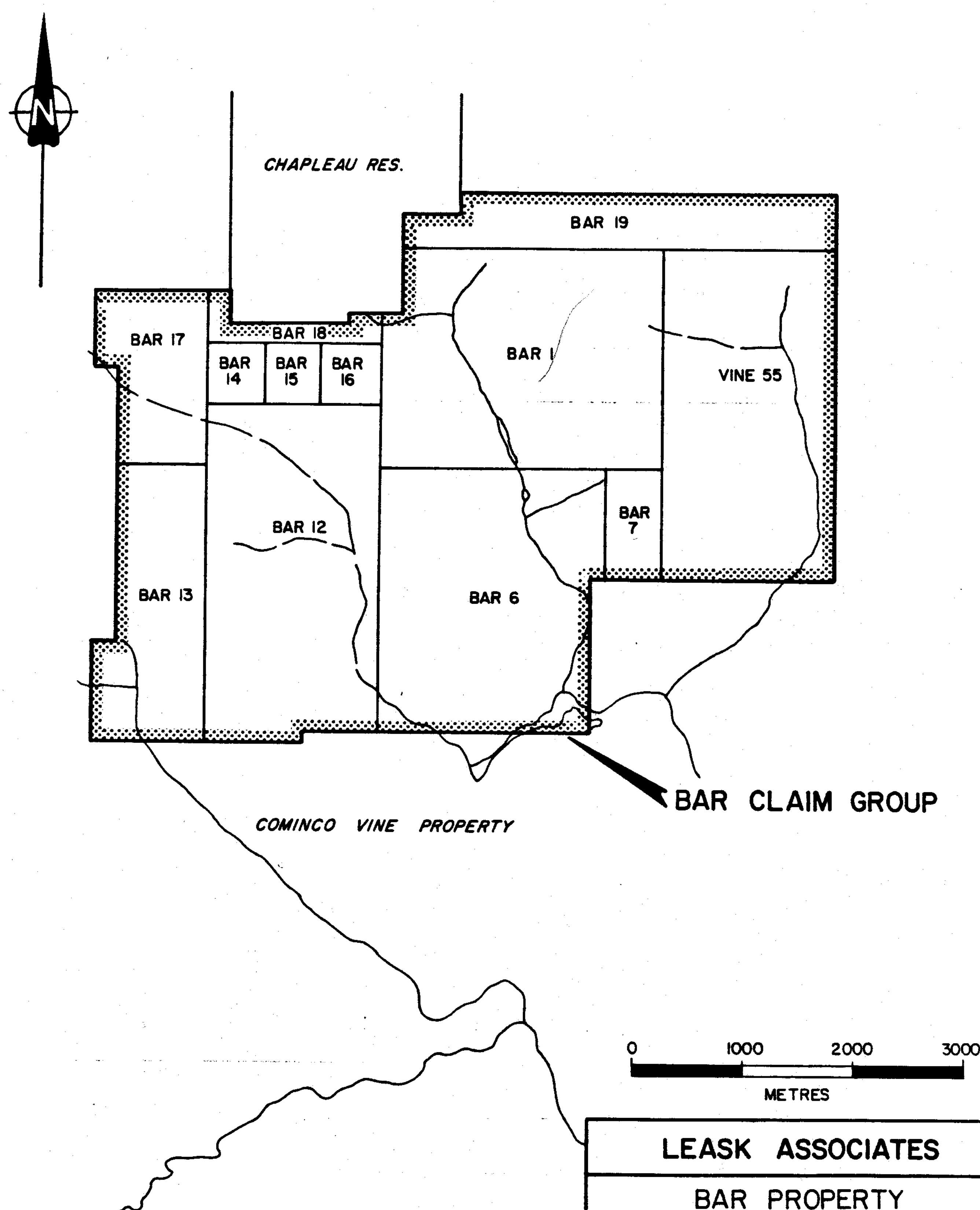

LEASK ASSOCIATES

BAR PROPERTY

CLAIM LOCATION MAP
Fort Steele M.D., B.C.

DATE: SEPT., 1987	SCALE: 1 : 50,000
NTS: 82G/5W	FIG. No.: 2

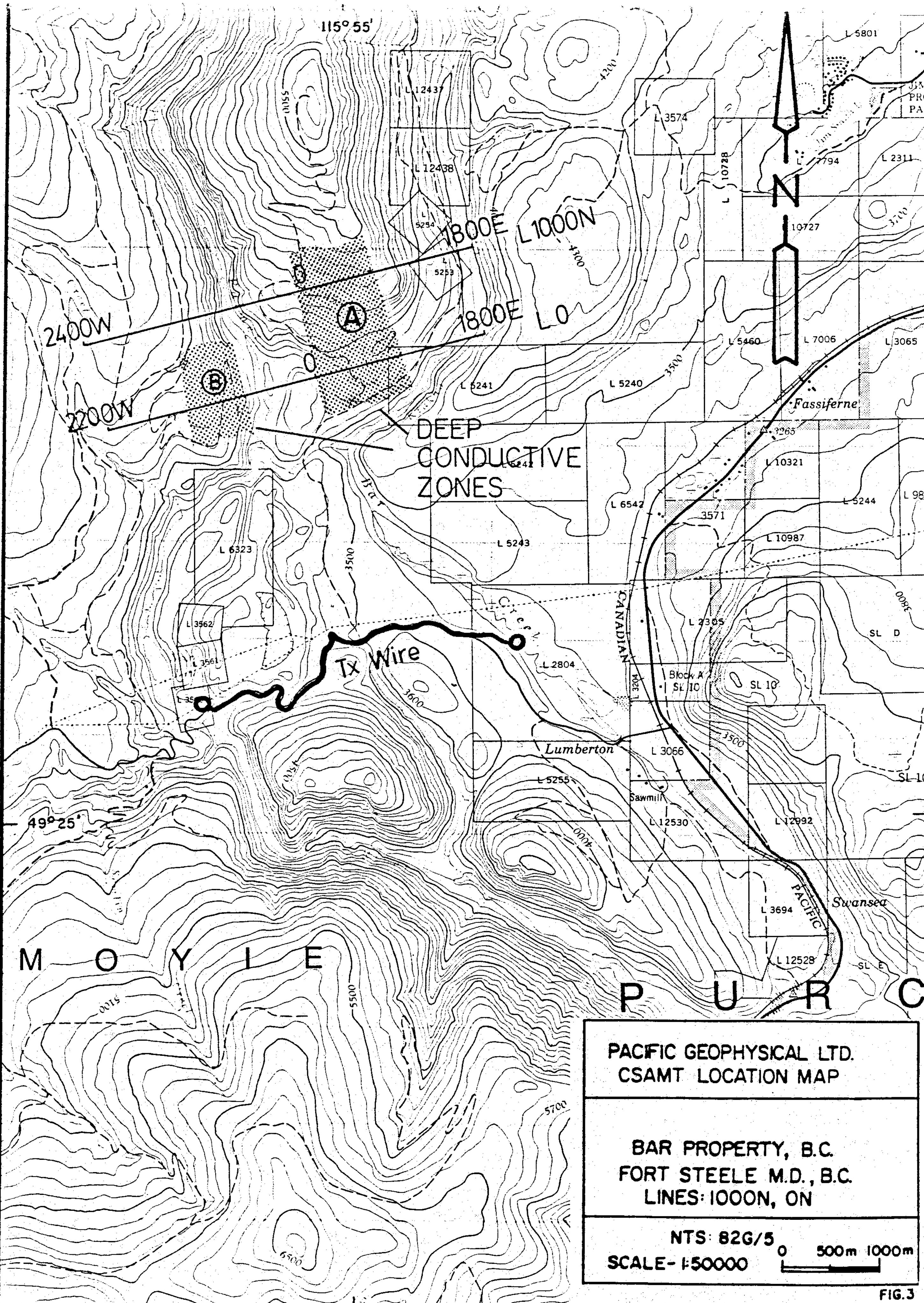

115° 55'
N
49° 25'
L1000N
1800E
L 0
1800E
2400W
2200W
A
B
DEEP CONDUCTIVE ZONES
Tx Wire
Lumberton
Sawmill
Fassiferne
Swansea
CANADIAN
PACIFIC
Bar
Creek
M O Y I E
P U R C
L 12437
L 12438
L 3574
L 5801
L 2311
L 7794
L 10728
L 10727
L 5254
L 5253
L 5460
L 7006
L 3065
L 5241
L 5240
L 6242
L 6542
L 10321
L 5244
L 10987
L 5243
L 6323
L 3562
L 3561
L 2305
L 2804
Block A
SL 10
L 3204
L 3066
L 5255
L 12530
L 12992
L 3694
L 12528
SL D
SL E
3571
3265
PACIFIC GEOPHYSICAL LTD.
CSAMT LOCATION MAP
BAR PROPERTY, B.C.
FORT STEELE M.D., B.C.
LINES: 1000N, 0N
NTS: 82G/5
SCALE- 1:50000
0 500m 1000m

FIG.3

3. DESCRIPTION OF GEOLOGY

The geology of the Bar Claim Group is illustrated on the GSC map 11-1960

The property is underlain by the Aldridge Formation which is a Precambrian massive grey quartzite and siltstone with thinly laminated argillites and siltstones dominating the upper part.

Structurally, the property is part of a major thrust block. To the Southeast, the block is bounded by the northeasterly striking Moyie reverse fault that dips steeply to the northwest. The block is bounded in the north west and the north similary by the Palmer Bar fault and the Cranbrook fault respectively.

The sulphide potential of the Aldridge Formation is illustrated 30 km to the north at Kimberley where Sullivan mine ore is mined at the middle-lower Aldridge horizon.

4. PRESENTATION OF DATA

The CSAMT resistivity results are displayed on the data plots as apparent resistivity vs. frequency pseudo-sections. It should be made clear that this presentation cannot be viewed as a true section of earth resistivity, particularly in the vertical direction, i.e. top of section to bottom of section, as the depth of penetration is dependent upon the resistivities encountered as well as the frequency employed to make the measurement.

Drawing No. 5887-1 shows the CSAMT resistivity data that has been corrected for the position of the transmitter wire relative to the survey lines (near field correction). Dwg. No. 5887-2 illustrates the uncorrected CSAMT resistivity data.

Also enclosed with this report is Dwg. No. A.M.T. 2020, a plan map of the Bar Property CSAMT grid at a scale of 1:10,000. The definite, probable, and possible CSAMT conductivity anomalies are indicated by bars, in the manner shown in the legends, on this plan map as well as on the corrected CSAMT pseudo-section, Dwg. No. 5887-1. These bars represent the interpreted surface projection of the deep anomalous zones.

5. DISCUSSION OF RESULTS

Two separate zones of anomalously high conductivity are interpreted to be present in the area evaluated by the present Controlled Source Audio Magnetotelluric (CSAMT) survey. These features are marked in plan form on Dwg. No. A.M.T. - 2020, and in pseudo section form on Dwg. No. 5887-1. Each trend is discussed separately below.

ZONE A

This zone is interpreted to strike across both Line 0 and Line 1000N, in the area just east of the Baseline 00. Width of the feature is thought to be in the order of 700 meters to 900 meters.

One dimensional computer inversions have been used to better estimate the depth to the conductive source, which is indicated to be relatively flat lying. Prior to calculating the inversions, data was first corrected for the position of the transmitter wire (near-field correction), and then "static shifted" to minimize the effect of near surface conductivity variations. This latter operation used the data recorded over Zone B as a guide, in that the source of Zone B is thought to have been tested by a previously drilled hole located south of Line 0. Conductive metallic mineralization was encountered in this diamond drill hole at approximately 1500 meters sub surface.

Figure 5 and Figure 6 show inversion outputs utilizing data recorded over Zone A on Line 0 and Line 1000N respectively. The former calculation estimates a depth of approximately 1500 meters to the target conductor, while the latter, more northerly inversion, returns a depth of approximately 1650 meter subsurface. It should be noted that one would expect a somewhat greater depth than 1650 meters to

PALMER BAR CSAMT Line 0 Stn 1100W

FINAL RESULTS FROM INVERSION

Rho1	Rho2	Rho3	Rho4	Rho5	Thk1	Thk2	Thk3	Thk4
2500.0	100.0	1500.0	100.0	700.0	250.0	51.4	1264.2	155.9

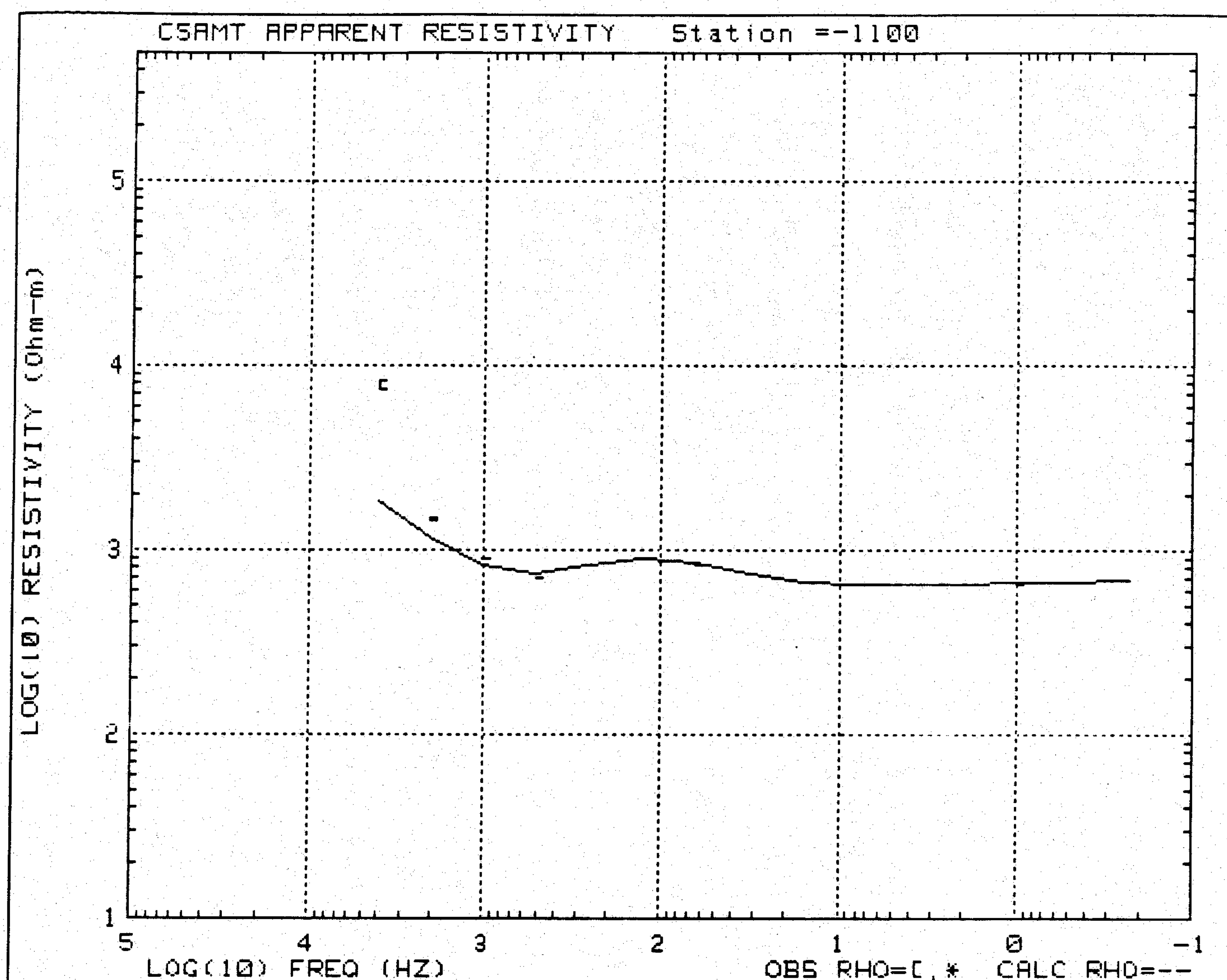

CSAMT SOUNDING DATA

F(Hz)	Obs Rho	Cal Rho	Pctdif	Wts	Obs Pha	Cal Pha	Phadif	Wts
4096.000	7851.1	1845.4	76.5	0	0.0	64.1	-64.1	0
2048.000	1469.6	1178.4	19.8	0	0.0	63.7	-63.7	0
1024.000	904.2	833.9	7.8	1	0.0	57.7	-57.7	0
512.000	710.3	740.5	-4.3	1	0.0	49.2	-49.2	0
256.000	830.0	824.2	.7	1	0.0	44.7	-44.7	0
128.000	896.2	900.9	-.5	1	0.0	46.5	-46.5	0
64.000	831.6	842.2	-1.3	1	0.0	49.6	-49.6	0
32.000	740.3	738.6	.2	1	0.0	50.1	-50.1	0
16.000	671.5	672.0	-.1	1	0.0	48.5	-48.5	0
8.000	644.5	646.7	-.3	1	0.0	46.7	-46.7	0
4.000	654.6	645.1	1.4	1	0.0	45.4	-45.4	0
2.000	652.2	653.2	-.2	1	0.0	44.7	-44.7	0
1.000	658.0	663.4	-.8	1	0.0	44.4	-44.4	0
.500	668.2	672.7	-.7	1	0.0	44.4	-44.4	0
.250	685.1	680.1	.7	1	0.0	44.5	-44.5	0

Fig. 4

PALMER BAR CSAMT Line 0 Stn 700 E

FINAL RESULTS FROM INVERSION

Rho1	Rho2	Rho3	Rho4	Rho5	Thk1	Thk2	Thk3	Thk4
2500.0	130.0	1500.0	75.0	800.0	230.0	57.3	1242.6	161.1

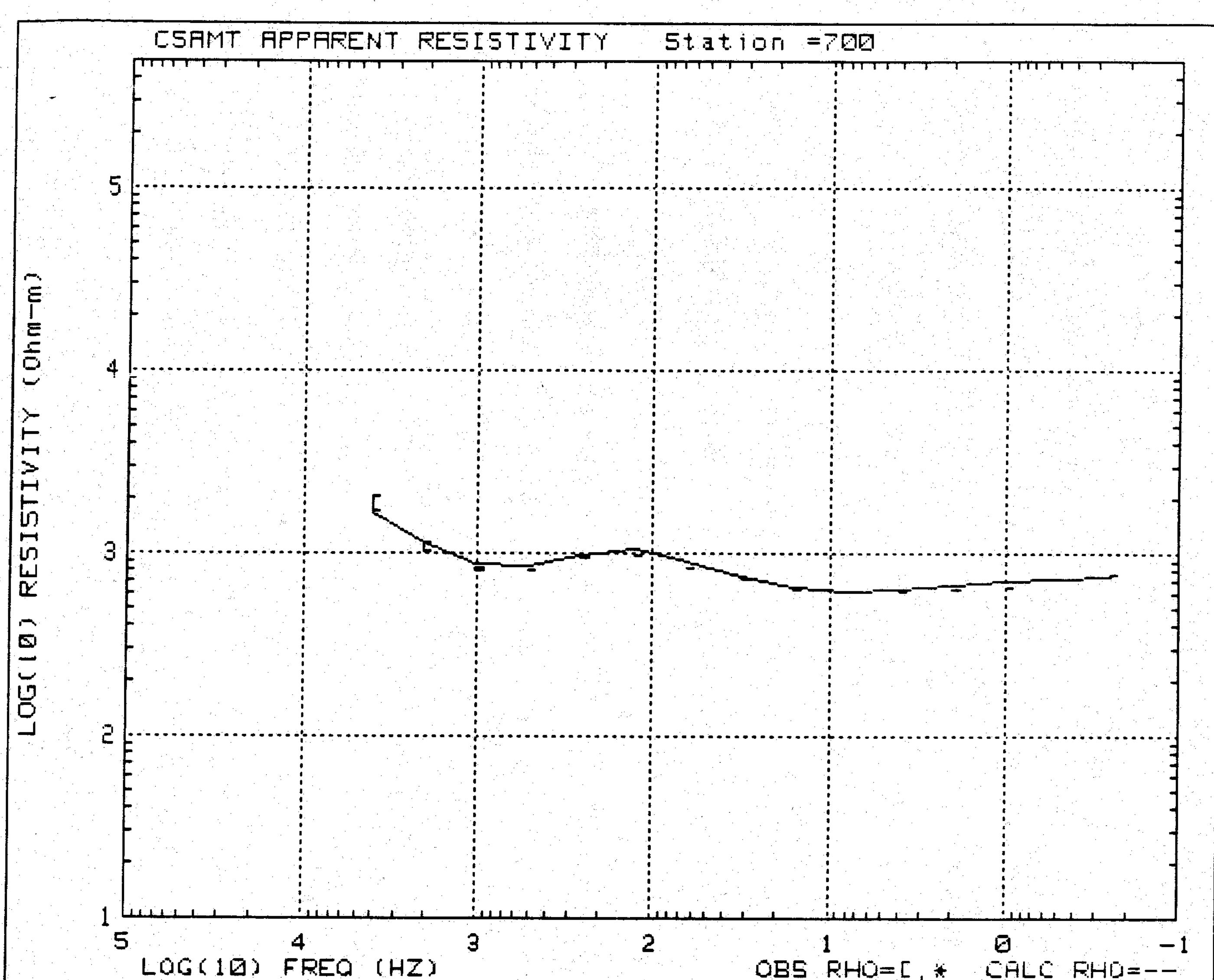

CSAMT SOUNDING DATA

F(Hz)	Obs Rho	Cal Rho	Pctdif	Wts	Obs Pha	Cal Pha	Phadif	Wts
4096.000	1874.2	1689.6	9.8	1	0.0	63.7	-63.7	0
2048.000	1082.0	1114.2	-3.0	1	0.0	61.8	-61.8	0
1024.000	814.1	838.3	-3.0	1	0.0	55.1	-55.1	0
512.000	806.7	797.1	1.2	1	0.0	47.2	-47.2	0
256.000	954.2	921.9	3.4	1	0.0	44.5	-44.5	0
128.000	962.0	980.2	-1.9	1	0.0	48.4	-48.4	0
64.000	833.1	851.7	-2.2	1	0.0	52.3	-52.3	0
32.000	716.7	700.2	2.3	1	0.0	51.9	-51.9	0
16.000	642.6	622.2	3.2	1	0.0	48.9	-48.9	0
8.000	617.7	607.7	1.6	1	0.0	45.8	-45.8	0
4.000	624.7	627.2	-.4	1	0.0	43.8	-43.8	0
2.000	630.2	659.0	-4.6	1	0.0	42.9	-42.9	0
1.000	654.2	691.2	-5.7	1	0.0	42.8	-42.8	0
.500	724.7	718.9	.8	1	0.0	43.0	-43.0	0
.250	761.0	740.7	2.7	1	0.0	43.4	-43.4	0

Fig. 5

PALMER BAR CSAMT Line 1000N Stn 300 E

FINAL RESULTS FROM INVERSION

Rho1	Rho2	Rho3	Rho4	Rho5	Thk1	Thk2	Thk3	Thk4
2500.0	150.0	1200.0	41.2	500.0	450.0	77.6	1132.0	138.8

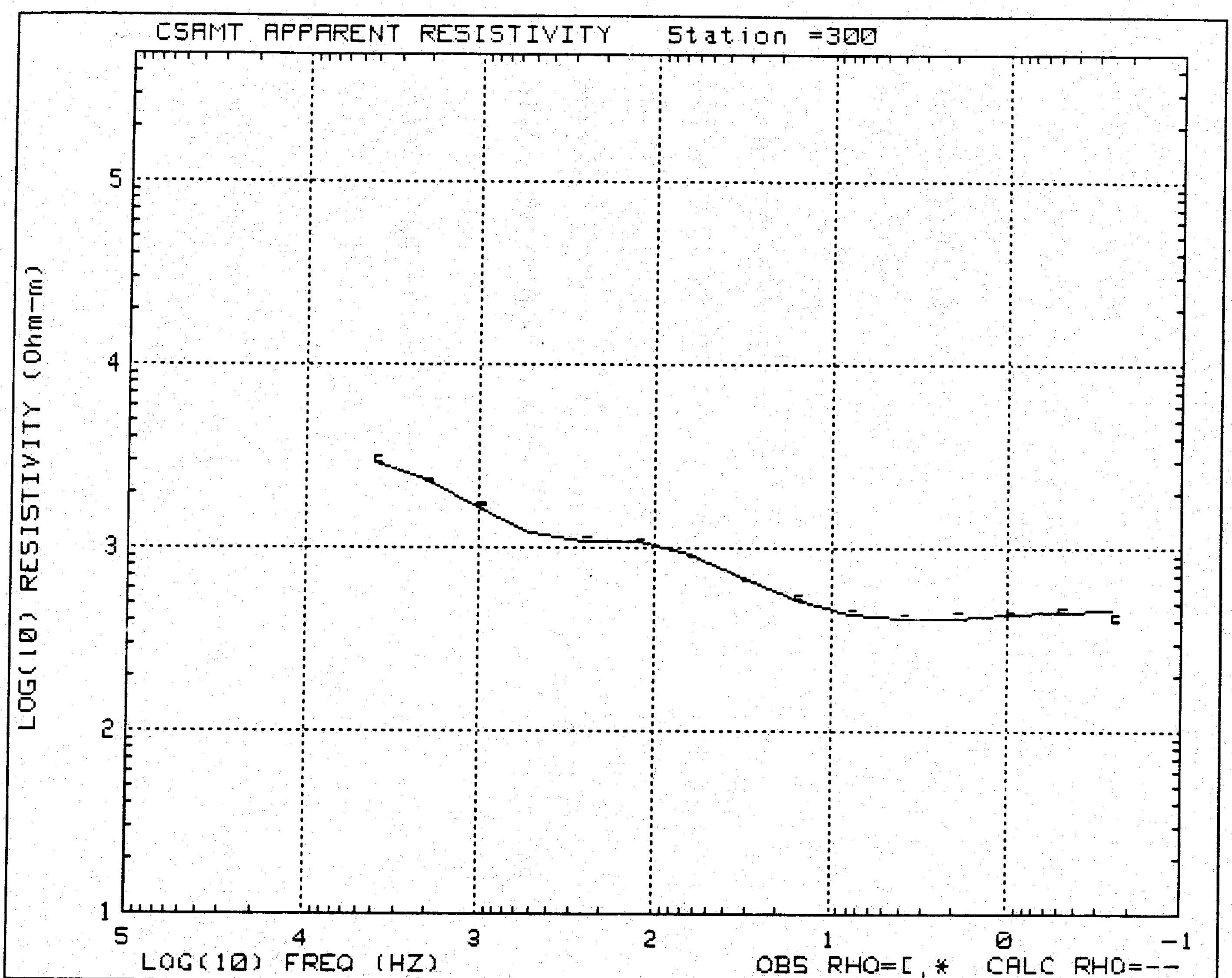

CSAMT SOUNDING DATA

F(Hz)	Obs Rho	Cal Rho	Pctdif	Wts	Obs Pha	Cal Pha	Phadif	Wts
4096.000	3042.9	2890.9	5.0	1	0.0	50.8	-50.8	0
2048.000	2322.7	2374.4	-2.2	1	0.0	58.1	-58.1	0
1024.000	1722.2	1668.8	3.1	1	0.0	60.5	-60.5	0
512.000	1196.8	1228.6	-2.7	1	0.0	57.1	-57.1	0
256.000	1149.5	1120.1	2.6	1	0.0	52.6	-52.6	0
128.000	1111.8	1104.6	.6	1	0.0	54.0	-54.0	0
64.000	900.3	920.9	-2.3	1	0.0	58.1	-58.1	0
32.000	676.0	682.3	-.9	1	0.0	58.9	-58.9	0
16.000	544.4	527.7	3.1	1	0.0	55.9	-55.9	0
8.000	455.9	457.1	-.3	1	0.0	51.6	-51.6	0
4.000	438.2	436.0	.5	1	0.0	47.9	-47.9	0
2.000	445.0	438.1	1.5	1	0.0	45.7	-45.7	0
1.000	453.3	448.5	1.1	1	0.0	44.5	-44.5	0
.500	462.9	460.2	.6	1	0.0	44.1	-44.1	0
.250	421.1	470.4	-11.7	1	0.0	44.0	-44.0	0

Fig. 6

the conductor under Line 1000N due to a combination of a shallow northerly dip, and rising topography towards the north. A possible cause of this descrepancy is uncorrected near surface resistivity variations, or the fact that the target is not really a one dimensional body.

ZONE B

Zone B is interpreted to only underlie Line 0, with the response being centered at approximately Station 1100W.

As was mentioned above, a previously completed vertical diamond drill hole, located roughly 700 meters south of the position of Zone B on Line 0, has intersected relatively conductive metallic mineralization at a depth of 1500 meters below the surface. This mineralization occurs at or just below the Sullivan mine horizon, and is probably the source of CSAMT Zone B.

Inversion of the near field corrected and static shifted data from Station 1100W on Line 0 is illustrated by Figure 4. A depth of approximately 1550 meters is calculated to the source of Zone B. This same inversion suggests that the Zone B conductor is not as conductive and/or thick as the source of Zone A.

SUMMARY OF RESULTS AND RECOMMENDATION

A controlled source audio magnetotelluric (CSAMT) survey has been carried out over the southern portion of the Bar Property, located approximately 12 kilometers southwest of Cranbrook, B.C. Two roughly east-west striking lines were traversed, as illustrated by Figure 3.

The CSAMT method is a technique whereby the resistivity of the earth can be determined by measuring horizontal and orthogonal electric and magnetic fields at a relatively large distance away from a long, grounded wire carrying an alternating current. Penetration depth is varied by changing the frequency of the transmitted signal. By selecting a suitably low range of frequencies, one can detect large conductors buried at great depths.

In the case of the Bar Property, two deep seated zones of enhanced conductivity can be seen in the CSAMT data sections. The locations of the zones are marked on Figure 3. Zone B, the less anomalous of the two trends, is detected only under Line 0, at a point roughly 700 meters north-northwest of a deep drill hole that reportedly encountered the target Sullivan horizon at approximately 1500 meters downhole. As this depth is consistant with the interpreted burial depth of the source of Zone B, it is possible that this part of the CSAMT data is outlining the moderately conductive, but uneconomic metallic mineralization intersected just below the Middle Aldridge-Lower Aldridge conformity (Sullivan horizon) by the previously mentioned drill hole.

The source of Zone A is indicated to be buried at a similar depth as that which gives rise to Zone B, however, the source of CSAMT Zone A appears to be a more conductive and/or thicker target.

In addition, this latter trend exhibits greater apparent width and length, with the zone being detected under both survey lines.

Therefore, CSAMT Zone A could represent the surface expression of a large, deeply buried sulphide body, and diamond drilling is recommended to physically test the source of the CSAMT response. A vertical drill hole collared north of Line 0, in the center of Zone A, should be considered.

PACIFIC GEOPHYSICAL LIMITED

Paul A. Cartwright

Paul A. Cartwright, P. Geoph.
Geophysicist.

Dated: January 15, 1987

7. ASSESSMENT DETAILS

Property: Bar Claim Group

Mining Division: Fort Steele

Sponsor: JOHN M. LEASK

Province: British Columbia

Location: 13 km. southwest of Cranbrook, B.C.

Type of Survey: Controlled Source Audio Magnetotelluric (CSAMT)

Operating Man Days: 38

Date Started: September 23, 1987

Consulting Man Days: 8

Dated Finished: October 2, 1987

Drafting Man Days: 4

Number of Stations: 4

Total Man Days: 50

Number of Reading: 615

Km of Line Surveyed: 8.2

Consultant:

P.A. Cartwright, 4238 West 11th Avenue, Vancouver, B.C.

Field Technicians:

R. Bulger, 224 - 17th Street, North Vancouver, B.C.
P. Mullan, 1440 Sandhurst Place, West Vancouver, B.C.
B. Counts, 4131 West 16th Avenue, Vancouver, B.C.

Draughtsman

B. Counts, 4131 West 16th Avenue, Vancouver, B.C.

PACIFIC GEOPHYSICAL LIMITED

Paul A. Cartwright

Paul A. Cartwright, P. Geoph.
Geophysicist

Dated: January 15, 1988

8) STATEMENT OF COSTS

Controlled Source Audio Magnetotelluric Survey
Bar Property, Cranbrook, British Columbia

Period: September 23, 1987 to October 2, 1987
Crew: P. Cartwright, B. Counts, R. Bulger, P. Mullan

9 1/2 Operating Days @ $1,450.00	$13,775.00
Mobilization-Demobilization	2,500.00
Report Preparation	2,000.00
	$18,275.00

PACIFIC GEOPHYSICAL LTD.

Paul A. Cartwright

Paul A. Cartwright, P. Geoph.
Geophysicist.

Dated: January 15, 1988

9. CERTIFICATE

I, Paul A. Cartwright, of the City of Vancouver, Province of British Columbia, do hereby certify:

1. I am a geophysicist residing at 4238 W. 11th Ave., Vancouver, B.C.

2. I am a graduate of the University of British Columbia, with a B.Sc. Degree (1970).

3. I am a member of the Society of Exploration Geophysicists, the European Association of Exploration Geophysicists and the Canadian Society of Exploration Geophysicists.

4. I have been practising my profession for 17 years.

5. I am a Professional Geophysicist licensed in the Province of Alberta.

6. I have no direct or indirect interest, nor do I expect to receive any interest, directly or indirectly, in the property or securities of Tectono Resources Ltd., Therm Resources Ltd. or any affiliates.

7. Permission is granted to use in whole or in part for assessment and qualification requirements but not for advertising purposes.

DATED AT VANCOUVER, BRITISH COLUMBIA this 15th day of January, 1988.

Paul A. Cartwright

Paul A. Cartwright, P. Geoph.

PART C

CSAMT CASE HISTORIES WITH A MULTI-CHANNEL CSAMT SYSTEM AND DISCUSSION OF NEAR-FIELD DATA CORRECTION

by

Mitsuru Yamashita, M.Sc.,

and

Philip G. Hallof, Ph.D.,

Paper presented at the
55th SEG Annual Convention
Washington, D.C.
October 1985

ABSTRACT

A Controlled Source Audio-frequency Magneto-telluric (CSAMT) system has been successfully developed utilizing initially, a Phoenix 6-channel, IPV-3 spectral IP receiver and IPT-1 (AC3003 model) transmitter. The CSAMT system now manufactured by Phoenix includes the microprocessor controlled V4, 8-channel receiver, with magnetic sensor coil and IPT-1 (AC3004 model) DC-10 kHz transmitter. The system has been used successfully in several test surveys and numerous field surveys.

In standard operation, six E-field magnitudes and one H-field magnitude are simultaneously measured at 16 binary related frequencies (0.25 to 8192 Hz). The controlled signal source is the IPT-1 transmitter, which drives current through a grounded, long-wave bipole. This generates an electromagnetic field at the same frequencies. The transmitter bipole is located several kilometers from the area to be surveyed. A large trapezoidal survey area, on either side of the transmitter bipole, can be covered from a single transmitter setting. This makes the CSAMT technique very cost-effective for mapping.

Apparent resistivities are calculated in real time for the six E-dipole sounding locations, at each of the 16 frequencies. All the measured and calculated data are stored in RAM memory, listed on a pocket printer, through a parallel I/O, and/or transferred to a mass storage device through a RS232 serial I/O, at the measuring site. Phase, E-field, H-field and the standard deviations are also measured and stored.

Later in a field base camp, the data are dumped into a field computer and processed automatically to generate an apparent resistivity pseudo-section plot. A near-field correction is also applied. A 1-D inversion program has also been developed for the field computer.

INTRODUCTION

The CSAMT method was introduced by Goldstein (1971) and Goldstein and Strangway (1975) to overcome problems encountered by the Audio Magnetotelluric (AMT) and Magnetotelluric (MT) methods.

The MT method is a well known exploration technique, used widely in hydrocarbon and geothermal exploration. MT measures fluctuations in the earth's natural electric and magnetic fields, in a broad range of frequencies between about .0001 Hz and 100 Hz. When the measurements are made in the audio-frequency range (10 Hz to 20 kHz) the method is known as Audio-frequency Magnetotellurics (AMT). Neither MT nor AMT requires a man-made power source. However, these advantages are often negated by the low magnitude and high variability of the natural signals.

The advantages of the controlled source method are several:

1. Signals are stronger, therefore the sensing equipment does not need to be as sensitive as that for MT or AMT.

2. Because of the coherent signal, the usual signal processing and enhancement technique are far more effective.

3. Thus CSAMT surveys can be much faster than AMT surveys.

One disadvantage with respect to the natural field mode is the nearness of the signal source. In the natural field methods, the signal source is, in effect, infinitely distant. This "plane wave" assumption simplifies both the mathematics of the technique and the interpretation of AMT/MT data. When a controlled source is used, the "plane wave" assumption is no longer true (at least not close to the transmitter), and the calculated apparent resistivity must be corrected for the "near-field" effect.

This system, fully utilizing the multi-channel, multi-frequency, microprocessor controlled instrumentation technology developed by Phoenix, results in rapid data acquisition as well as producing a CSAMT system that has improved further on the above CSAMT advantages.

SYSTEM CONCEPTS

i) CSAMT Parameters Measured and Calculated

Both the electric field (E-field) and the magnetic field (H-field) are measured, at the frequency transmitted from the remote transmitter bipole source. The magnitudes of both the E-field and H-field are determined, as well as their relative phase. The measured data are digitally stacked, filtered and processed in real-time; the apparent resistivity is also calculated at each frequency. This calculation is made using the following Cagniard equation and the phase difference.

$$\rho_a \approx \frac{1}{5f}\left|\frac{E_x}{H_y}\right|^2 \; ; \; \phi = \phi_E - \phi_H \qquad (1)$$

where ρ_a is apparent resistivity in ohm-m; f is frequency in Hz; Ex is the E-field magnitude, in mv/km, parallel to the transmitter dipole; Hy is H-field magnitude perpendicular to the E-dipole in gammas; ϕ is phase difference in radians; ϕ_E is E-field phase and ϕ_H is H-field phase.

In addition to the parameters mentioned above, the standard deviations of each parameter, $|Ex|$, $|Hy|$, ρ_a, ϕ_E and ϕ_H, are calculated for signal verification.

ii) Receiver System

The CSAMT receiver system consists of the V4 receiver console, a magnetic sensor coil and peripherals. Photo 1 shows a V4, eight-channel universal receiver which can be used for spectral IP, conventional IP in time or frequency domain, and CSAMT. Photo 2 shows the magnetic sensor coil used to measure the H-field. Non-polarizable electrodes are usually employed for the E-dipoles, to measure the E-field.

The main features of the V4 receiver are:

1. Simultaneous measurement of eight input channels.
2. Microprocessor-controlled, real-time filtering, signal stacking and averaging.
3. Data logging in solid state, non-volatile memory.
4. Two standard output ports (parallel and serial) for a vest pocket printer and data transfer to a microcomputer.
5. Automatic gain control and self-potential (SP) cancellation.
6. Frequency range from 0.25 to 8192 Hz for CSAMT operation.
7. Real-time calculation of apparent resistivity, phase, mean and standard deviation of measured parameters.
8. Continuous monitoring of any measured and calculated parameters on 4 line x 16 characters LCD display.
9. Comprehensive keyboard-and-prompt operation.

iii) Transmitter System

The CSAMT transmitter system consists of a transmitter console, a frequency control device, a motor generator and peripherals. Photo 3 shows an IPT-1 transmitter console. For the transmitter bipole, a long magnet wire is laid on the ground, in an approximate straight line. Both ends are grounded.

The main features of the transmitter system for the CSAMT operation are:

1. Frequency range from 0.25 to 8192 Hz, with a binary step.
2. Output voltage of up to 800 volts.
3. Maximum continuous output power of 3kw, with MG-3 motor generator.
4. Regulated current up to 10 amperes.
5. Automatic turn-off protection if the current exceeds 150% full scale or if it is less than 5% full scale.

The transmitter system is portable. Furthermore the transmitter system can be situated at one location to cover a large survey area. There are more powerful transmitter systems available from Phoenix for applications where portability is not the most important factor. Depending upon the frequency range required these systems can have a power output of 30 kva, up to 100 kva.

iv) Survey Configuration and Grid

Figure 1 illustrates the survey configuration and grid. The standard configuration performs Six (or Seven) Ex-field and One Hy-field measurements at each of 16 frequencies, (0.25 to 8192 Hz). As illustrated, the E-fields are measured with a dipole using non-polarizable electrodes, in the same way as for IP measurements. The survey traverse line, for the series of equally spaced E-dipoles, is parallel to the transmitter bipole. The measurement dipole length is determined by the desired scale of the survey; this may also be influenced by the E-field signal strength, which is in turn determined by the transmitter-receiver distance, the transmitter bipole current and the earth resistivity. The receiver dipole length may be in the range from 10 meters to 200 meters.

A horizontal magnetic sensor coil is placed on the ground, approximately at the centre of the series of E-dipoles. It must be placed several meters away from the E-dipole line and the receiver console, to avoid interference, as well as to reduce inductive coupling due to operator movement. Only one H-field measurement is required for each group of six E-field measurements; the justification for this will be discussed later.

The transmitter (powered by a suitable motor generator) sends current into a long wire, grounded bipole. The length of the bipole may be varied from several hundred meters to several km, depending upon signal strength requirement. This will also be discussed later, as will be the transmitter-receiver distance and the survey area to be covered with one transmitter bipole location.

CSAMT SIGNALS AND PARAMETERS

i) Field Strength

At a given receiver location, the field strength depends upon various factors: location of measuring point (relative to Tx bipole), transmitter bipole length, current in the bipole, earth resistivity and measuring frequency. It is important to know the approximate field strength to be expected, in order to plan the survey grid and to locate the transmitter properly, to give the optimum survey results.

Figure 2(a) and Figure 2(b) show examples of contours of the Hy-field strength and Ex-field strength at 1024 Hz, over a homogeneous earth of 1000 ohm-m, based on the parameters indicated in the diagram. The heavy dashed contours indicate the region beyond which the field strength becomes minimal in magnitude.

ii) Apparent Resistivity

The apparent resistivity is calculated from the ratio of the electric field and magnetic field magnitude using the well known Cagniard equation (1) for MT. It should be noted that this Cagniard equation is exactly valid only in the plane wave region of the electromagnetic field; i.e., when the distance between transmitter signal source and receiving location is sufficiently large.

Figure 2(c) indicates the apparent resistivity, calculated by the Cagniard equation over a homogeous earth of 1000 ohm-m using the field strength magnitudes shown in Figure 2(a) and Figure 2(b). It should be observed that the valid area for the application of the equation is indicated by the calculated apparent resistivity value of approximately 1000 ohm-m, which is equal to the true resistivity value. The dashed line depicts the plane of the minimal field strength previously mentioned and measurements in this area should be avoided.

The effective survey area, a trapezoidal shape, indicated in Figure 2(c) is thus optimally placed within the maximum possible field strengths and by avoiding areas that are too close to the transmitter bipole.

iii) Far-field and Near-field

In a CSAMT survey, the distance between the transmitter and receiver locations is constrained, in general, by the requirement that the magnetic field and the electric field be strong enough to permit useful measurements. The paradox encountered is that where the "plane wave" assumption is valid, the signal may be weak; and where the signal is strongest (near the transmitter), the "plane-wave" assumption is no longer valid.

At some distance from the transmitter bipole, where the transmitted electromagnetic field becomes a "plane-wave", it is called "far-field". The Cagniard equation is valid in the "far-field" situation for the calculation of the apparent resistivity. The "far-field" distance, L_f, is approximately given by the following equation:

$$L_f \quad > \quad 3 \text{ x skin depth} \approx 1509\sqrt{\rho/f}$$

where L_f is in meters, ρ is the resistivity of the homogeneous earth in ohm-m and f is frequency in Hz.

If the distance between transmitter and receiver is much less than L_f, the transmitted field is not "plane-wave" in character; it is referred to as the "near-field". In the "near-field", the Cagniard equation overestimates the actual resistivity. Figure 3(a) shows the apparent resistivity curve, using the Cagniard equation with theoretically calculated Ex and Hy values, over a homogeneous earth. The apparent resistivity curve in the "near-field" is characterized by a slope of 45 degrees, meaning that the apparent resistivity value is doubled by each binary frequency step. The area of the gradual change from "far-field" to "near-field" is called the "transition-zone" or the "transition-field".

Figure 4(a) shows Hy-field vs frequency over a homogeneous earth, for various resistivity and transmitter-receiver distance. The Hy-field can be expressed by the following equations:

$$\text{in "far-field"; } Hy \simeq \frac{1}{\sqrt{\sigma f}\cdot r^3} \qquad (2)$$

$$\text{in "near-field"; } Hy \simeq \frac{1}{r^2} \qquad (3)$$

where $\sigma = 1/\rho$ is conductivity in mhos/m.

Figure 4(b) shows Ex-field vs frequency in the same manner. The Ex-field can be expressed by the following equations:

$$\text{in "far-field"; } Ex \simeq \frac{1}{\sigma r^3} \qquad (4)$$

$$\text{in "near-field; } Ex \simeq \frac{1}{\sigma r^3} \qquad (5)$$

For "far-field", from the equation (2) and the equation (4);

$$\frac{Ex}{Hy} \approx \frac{\frac{1}{\sigma r^3}}{\frac{1}{\sqrt{\sigma f}\cdot r^3}} \approx \sqrt{\frac{f}{\sigma}}$$

therefore,

$$\rho_a \approx \frac{1}{f}\left|\frac{Ex}{Hy}\right|^2$$

introducing factor, $K_f/5$

$$\rho_a = \frac{K_f}{5\cdot f}\left|\frac{Ex}{Hy}\right|^2 \qquad (6)$$

For "near-field", from the equation (3) and the equation (5),

$$\frac{Ex}{Hy} \sim \frac{\frac{1}{\sigma r^3}}{\frac{1}{r^2}} \approx \frac{1}{\sigma r}$$

therefore,

$$\rho_a \approx r\left|\frac{Ex}{Hy}\right|$$

introducing "near-field" factor K_n

$$\rho_a = K_n \cdot r \left|\frac{Ex}{Hy}\right| \qquad (7)$$

iv) First Order "Near-Field" and "Transition-Field" Correction

Figure 4 (d) shows the K_r and K_n factors vs $\left(f \times r \times \left|\frac{Ex}{Hy}\right|\right)$, for any uniform earth, for the entire resistivity, transmitter-receiver distance and frequency ranges. These are unexpectedly simple relationships. It should be noted that the K_n is a constant, 0.63 in the "near-field" and K_f is a constant, 1.0, in the "far-field", indicating that equation (6) is the same as the Cagniard equation. From the known values of f (frequency), r (transmitter-receiver distance) and [E/H] (measured), it is possible to categorize a particular field situation as "far-field", "transition-field" or "near-field", for any conditions encountered.

Now the corrected apparent resistivity can be calculated from the field measurements using: the Cagniard equation if the measurement is in the "far-field"; the equation (7), if the measurement is in the "near-field"; and the equation (6) or the equation (7), using proper K_f or K_n, values if the measurement is in the "transition-field".

If a valid "near-field" and "transition-field" correction is performed on CSAMT data (to obtain apparent resistivity values equivalent to the "far-field" situation), then the apparent resistivity value is equivalent to that for a scalar MT/AMT measurement. Consequently, well-developed existing interpretation techniques for MT can be utilized. Proper correction also prevents some false and dangerous interpretation errors, caused by the "near-field" and "transition-field" variations in the measured data.

v) Use of "Near-Field" Correction for Non-Uniform Earth

The use of the K_n and K_f parameters shown in Figure 4(d) results in a perfect correction to the measurement data for a uniform earth, to give the apparent resistivity that would be measured for the "far-field" situation. Our experience has been that this "first order" correction is excellent even in situations in which the earth is non-uniform.

Figure 4(c) indicates an example of the method executed on a field data curve automatically, by a micro-computer. The example shows the field data profile calculated from the Cagniard equation, as well as the curve for the "near-field" corrected apparent resistivity. The regions of "near-field", transition-field" and "far-field" are also indicated. After corrections, the low resistivity portion of the curve, designated by "A" on the uncorrected Cagniard resistivity profiles, was eliminated and the data indicate perhaps two layers of high resistivity over a low resistivity, instead of the high-low-high layered geometry.

The data shown in Figure 4(e) and Figure 4(f) pertain to a layered earth. The plots show the ρ_a vs f curves for specific subsurface geometries and several separations between the transmitter dipole and the measurement point. In these examples, the upper layer is more resistive than the lower layer.

In both examples the calculated Cagniard apparent resistivity for a measurement at a distance of 4.0 km has been corrected using the "near-field" correction program outlined above. In both examples, the corrected curve agrees exactly with the "plane-curve" or true Cagniard example.

The first order, "near- field" correction outlined above is not as perfect for the case in which the surface layer is more conductive than the lower layer. The theoretical results shown in Figure 4(g) are the near-field corrected data for one example. The corrected results are much closer in magnititude to the plane-wave data than the magnitudes that would be measured at four kilometers from the transmitter bipole. This type of data can be used by the geophysicist to give some feeling for the errors to be expected from the "near-field" corrected results.

DATA PROCESSING AND PRESENTATION

Survey data are measured, the parameters are calculated, stored in the RAM of the receiver unit and tranferred into permanent mass storage media (such as a cassette tape) at the end of each day, in the field base camp. The data can then be immediately processed by micro-computer. The field presentation of the results is in the form of a contoured apparent resistivity pseudosection plot or profile plot. Other parameters such as phase, or E and H field magnitude, can also be presented in the same form.

This immediate data processing and presentation permits the geophysicist to modify the survey plan and also to VERIFY DATA IN THE FIELD. A 1-D inversion program has also been developed for a micro-computer to use in the field base camp or in the office. Some examples will be shown in the discussions of specific case histories.

ADVANTAGES OF CSAMT AND PHOENIX SYSTEM

There is no geophysical exploration method and/or system that can be said to be superior to any other system and method, in respect of all situations. However, the following list describes some advantages of CSAMT in general, and of the Phoenix V-4 CSAMT system in particular.

1. Depth of detection.
   The depth of detection in geophysical exploration is not easy to express in simple terms. It is related to many factors, such as earth resistivity, frequency, size of target, resistivity contrast, background electrical noise, geological noise and system sensitivity. The effective depth of penetration in CSAMT is a function of frequency and earth resistivity, and not the length of the receiver dipole or the distance between transmitter and receiver. The frequency range of 0.25Hz to 8192 Hz permits sounding depths that vary from very shallow to very deep. The effective depth of detection of CSAMT, therefore, may be several

hundred meters to several kilometers, depending upon the characteristics of the conductor at depth.

2. Lateral resolution.
   CSAMT offers excellent lateral resolution, dependent only upon the length of the receive dipole, independent of the distance between the transmitter and receiver. The length of the receiver dipole can be adjusted to the size of the exploration target, with no loss in depth of penetration. A reconnaissance mode survey can often be completed using a large receiver dipole, typically 100m to 200m.

3. Flexible survey design.
   Normally a large survey area can be covered using a single grounded transmitter bipole. The location of this bipole, relative to the survey area, is often flexible enough to allow utilization of existing roads or trails to lay out the bipole wire and to position the transmitter equipment.

4. Little topographic effect between receiver and transmitter.
   Since the measured value is normalized at the receiver, the topographic relation between the transmitter and receiver is not an important factor. This fact makes CSAMT particularly useful in mountainous or remote regions, as well as within limited land holdings.

5. Ease of set-up of transmitter.
   The single grounded transmitter bipole is much easier to set up and maintain, than the large rectangular or square loops generally utilized by time-domain EM system. These loops must typically be several hundred meters to a few kilometers square.

6. Effects of transmitter location.
   The location of a large loop transmitter, for time-domain EM, is often critical to anomaly response. A second conductor can be easily masked by a first conductor located closer to the transmitter. Therefore, in time-domain EM, it is frequently necessary to repeat measurements with a second transmitter set-up at a different location from the first set-up. The limitations are discussed by Spies and Parker in Geophysics, Vol. 49, No. 7, page 902-912. CSAMT, on the other hand is much more independent of transmitter location, with a reasonable distance between transmitter and receiver. This is so, because CSAMT measures relative phase shift and amplitude ratio between the E and H fields. These parameters are controlled by the local resistivity surrounding the measuring point. Intervening conductors (between Tx dipole and Rx measuring point) affect the absolute phase shift/amplitude ration between Rx-Tx, which is not of interest in CSAMT.

7. Effective measurement points.
   With other EM and resistivity methods, to obtain satisfactory anomaly shape information, the measurements have to be performed on either side of the anomaly. Also, especially in Schlumberger method, the survey line must be extended to permit the transmitter bipole to extend to either side of sounding point, requiring extra

line cutting beyond a survey area. This is not the case for CSAMT, because each station is essentially a point sounding. Fewer receiver dipole measurements are required to represent an anomaly and no extra line cutting is required.

8. Apparent resistivity measurements in real-time.
   With other EM techniques, it is generally necessary to do data processing and interpretation after a survey is completed, in order to calculate the resistivity of the conductor and the host media. CSAMT provides real-time calculation of apparent resistivity, which helps the geophysicist to understand the situation immediately, and permits him to re-configure the survey, if needed.

9. High productivity through simultaneous multi-station measurements.
   Six (or optionally seven) E-field measurements and one H-field measurement are made simultaneously. Resistivity changes are predominantly reflected by changes in the E-field magnitude. Only one H-field measurement, per group of E-measurements, is needed because the H-field is essentially constant over significant distances along a line parallel to the transmitter dipole, even in the vicinity of very strong conductive features. Although survey progress will be dependent upon the topography of an area, seven receiver set-ups can be easily performed in a field day. This produces data from forty two stations, with sixteen frequencies, from 0.25 Hz to 8192 Hz, at each station.

10. Wide frequency range.
    The wide frequency range from 0.25 Hz to 8192 Hz, in binary steps, provides very shallow to very deep soundings, thus making the interpretations, especially with inversion, more effective.

EXAMPLES OF FIELD RESULTS

The CSAMT Method has been found to be very useful for the mapping of subsurface resistivities. As we shall see, the method is particularly useful in locating, and mapping, relatively small zones, at considerable depth. However, the scale of any particular survey is determined solely by the length of the E-field dipole employed. In our work, this distance has ranged from 25 meters to 200 meters.

The "near-field" and "transition-field" correction procedures described above have been used in all of the examples to be discussed. Our impression is that this simple "first-order" correction to the data does, in fact, produce results that approximate those that would be measured in the true "plane-wave" situation.

i) Nighthawk Lake Grid, Timmins, Ontario, Canada

The Nighthawk Lake Grid is located near Timmins, Ontario, in a region where the surface is covered by approximately 100 meters of glacial, lake-bed sediments. The deposit, itself, is an approximately horizontal source of sulphide and graphite.

The results shown in Figure 5(a) are the data measured by an E-field dipole of 25 meters. The measurements were made at a distance of 4.0 kilometers from the grounded current bipole. The effect of the conductive overburden layer and the bedrock conductor (centered at 1+50S to 0+50S) can both be seen in these uncorrected results. However, the effect of the "near-field" distortion can also be observed in the fact that the apparent resistivities, calculated using the Cagniard equation, increase sharply as the applied frequency is decreased.

The data shown in Figure 5(b) are those from the "near-field" corrected procedure completed by the micro-computer. The conductive surface layer (higher frequencies) is still present and the apparent resistivities measured at depth (lower frequencies) are approximately constant. The identical results were produced when the correction procedure was applied to data measured 7.6 kilometers from the current bipole.

The data shown in Figure 5(c) are scaler AMT results published by Strangway etal from measurements made on Line 1E. The lowest frequency used was 10 Hz, but the pseudosection is essentially the same as that for the CSAMT, corrected results.

ii) Line E Hatchobaru Grid, Ohita, Japan.

This line is from a geothermal survey near Ohita, Japan. The line was 5.8 kilometers from the transmitter current bipole and the E-field dipole length was 100 meters. The corrected data shown on Figure 6(a) indicate a layered media. The conductivity layer, at depth, is best detected in the range from 4.0 Hz to 1.0 Hz. These results have been interpreted using the one-dimensional inversion scheme we have developed for scaler AMT data. The inversion is performed at each sounding site, using a micro-computer in the base camp.

The results of these six inversions are shown in Figure 6(b). The interpreted true resistivity values, and the interpreted boundaries, shown by small rectangles, indicate an approximately layered earth. The conductive layer is centered at approximately 1000 meters of depth. The interpretation of the corrected CSAMT data agrees quite well with that previously developed by the joint inversion of MT data and Schlumberger resistivity data. (See boundaries and resistivity values designated by ellipses).

iii) Line C Hatchobaru Grid, Ohita, Japan.

This line is 400 meters from Line E. The results shown in Figure 7(a) suggest a more complex subsurface geometry than the layered earth indicated in Figure 6(a). The result of the one-dimensional interpretation procedure is shown in Figure 7(b). The subsurface geometry here is indicated to be more complex than on Line E; however, the conductive layer is still present.

The joint inversion of the previous MT and Schlumberger resistivity results also indicate the presence of the conductive layer, at depth.

However, the more complex geometry has resulted in greater differences between the CSAMT inversions and the MT inversion.

iv) Abuta Mine, Hokkaido, Japan.

The Test Line at the Abuta Mine passed directly over the Kuruko-type ore deposit. The massive sulphide zone lies at a depth of 50 to 75 meters, the host rocks are relatively conductive, relatively young volcanics. The position of the sulphide zone, and the corrected CSAMT apparent resistivity pseudosection are shown in Figure 8. Even within the environment of the low resistivity host rocks, the position of the deep conductor is clearly defined. The lateral resolution of the CSAMT measurement is excellent.

v) McLean Lake Deposit. Athabaska Area, Saskatchewan.

The uranium deposits at McLean Lake lie beneath approximately 550 feet of the younger, Athabaska sandstones. The specific geologic situation for these uranium deposits is well known, due to the considerable amount of drilling that has taken place. The uranium and sulphide orebodies are concentrated in zones of intense fracturing and alteration that modify the porous regolith that lies at the top of the pre-Cambrian unconformity.

The regolith itself might be expected to have a higher conductivity than the overlying Athabaska sandstones, or the pre-Cambrian basement. The overbodies have a relatively small cross-section; however, they are conductive enough to have caused electromagnetic anomalies in some previous surveys. The corrected CSAMT results shown in Figure 9(a) were measured using an E-field dipole of 200 feet, at a distance of 7.2 km from the transmitter current bipole.

The apparent resistivity pseudosection indicates a subsurface structure that agrees very well with the known geology. A discontinuous, poorly defined conductor extends across the entire one mile length of the line surveyed; this almost certainly represents the conductive regolith. The McLean North Zone, Pod #1 is centered at 13+00N to 14+00N. The McLean South Zone, East Pod is centered at 8+00S to 7+00S.

The positions of the uranium ore bodies both correlate with moderate magnitude, definite, resistivity lows, on the pseudosection on Figure 9(a). The results shown on Figure 9(b) were measured using a 100 foot E-field dipole. The resistivity lows from the orebodies are still clearly defined, even at a depth of more than 500 feet.

In addition, there are several narrow, shallow, local zones of low apparent resistivity that were not clearly evident in the measurements with the 200 ft E-Field dipole.

The measurements on Line 12E, 100 foot E-field dipole, are shown in Figure 9(c). At this location four hundred feet to the east, the orebodies are poorly developed. The two zones are centered at 12+50N and 9+50S to 8+50S. The apparent resistivity anomalies that correlate with these positions are also less definite on Line 12E than they were on Line 8E. However, these anomalies, and several other features on the pseudosections, can be correlated from line to line.

It is possible to solve the AMT scalar "Forward Problem" for a two-dimensional earth. The apparent resistivity vs frequency pseudosections generated by this procedure would be expected to be similar to those from "near-field" corrected CSAMT field results over linear conductors.

The forward problem solution shown in Figure 9(d) is for a subsurface geometry that approximates that at the McLean Lake Uranium Deposits. The contour pattern shown is very similar to several of those measured at McLean Lake. This is particularly true for the smoothed data measured using a 200 feet E-field dipole.

vi) Corey East Pinacle Reef, Enniskillen Township, Ontario.

Careful measurements with the CSAMT system can be used to locate,. and map, any subsurface structure that contains a resistivity contrast. The data shown on Figure 10 were measured over a small, petroleum producing, pinnacle reef in south-western Ontario. The measurements were made at a distance of 7.3 kilometers from the current bipole, using an E-field dipole of 100 meters.

From electric log measurements in the drill holes shown in Figure 10, the conducting features present would be expected to be the A-2 shale and the Salt Water beneath the oil.

An unusual, and quite definite apparent resistivity pattern on the pseudosection in Figure 10 correlates with the pinnacle reef. There is no obvious explanation for the apparent resistivity high that lies beneath (at lower frequencies) the conductive feature that appears to correlate with the reef.

CONCLUSIONS

The CSAMT method can be used to produce apparent resistivity pseudosections of the subsurface. The corrections that are necessary if the measurement point is near the transmitter current bipole can be automated using a microcomputer. This procedure results in apparent resistivity vs frequency pseudosections that are very similar to those that would be measured using a scaler AMT (plane-wave) technique.

Our limited experience, to date, has found several applications for the method and it is expected that others will follow.

ACKNOWLEDGEMENT

The development of the Phoenix V-4, CSAMT System was funded, in part, by an Exploration Technology Development Fund Grant from the Ministry of Natural Resources of Ontario in 1984 and 1985. The authors thank the personnel of the Ontario Geological Survey for various advice and assistance. The survey data included is shown with the permission of Kyushu Electric Power Co., Nittetsu Mining Co., Minatco Limited and Ram Petroleum Ltd. We appreciate their assistance.

REFERENCES

Cagniard L.,
1953: Basic Theory of the Magnetotelluric Method of Geophysical Prospecting. Geophysics 18, p. 605-35.

Goldstein, M.A.
1971: Magnetotelluric Experiments employing An Artificial Dipole Source. Unpublished Ph.D. Thesis, Department of Physics, University of Toronto.

Goldstein, M.A., and Strangway, D.W.
1975: Audio Frequency Magnetotelluric with a Grounded Dipole Source. Geophysics Vol. 40 p. 669-83.

Spies, B.R., and Parker, P.D.
1984: Limitations of Large-Loop Transient Electromagnetic Surveys in Conductive Terrains. Geophysics 49, p. 902-912.

Strangway, D.W., Ilkisik, O.M., and Redman, J.D.
1983: Grant 118, Surface Electromagnetic Mapping in Selected Portions of Northern Ontario, 1982-1983. Ontario Geological Survey Miscellaneous Paper 113.

Hy and Ex FIELD STRENGTHS CALCULATED for A UNIFORM EARTH EXAMPLE

Tx : L = 4 Km , R_W = 80 Ω , R_C = 100 Ω , R_T = 180 Ω , V = 800v , I = 4.4 A , P = 3.5 Kw
f = 1024 Hz , ρ = 1000 Ω-m , 3δ ≈ 1500 m

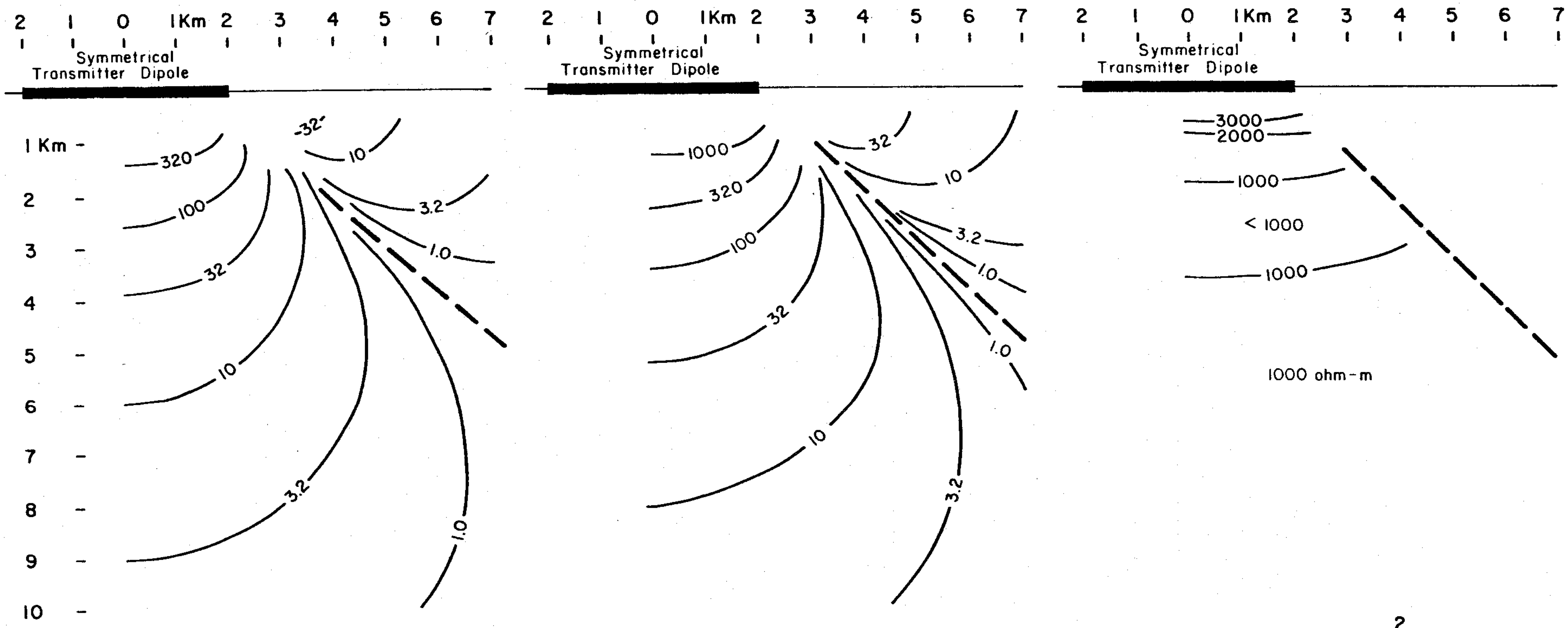

(a) Hy in mγ

(b) Ex in mV/Km

(c) $\rho_a = \frac{1}{5f}\left|\frac{Ex}{Hy}\right|^2$ in ohm-m

FIGURE 2

Phoenix V4 - CSAMT System

Survey Configuration and Grid

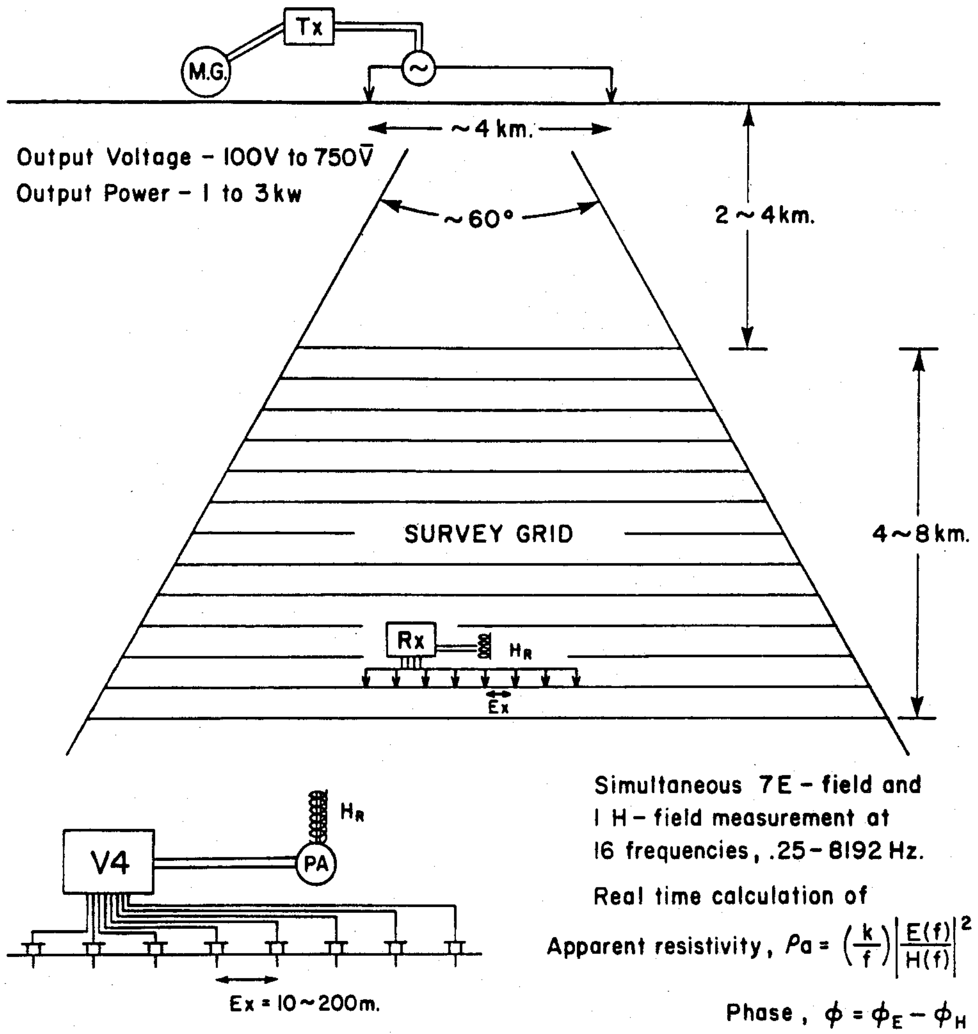

FIGURE 1

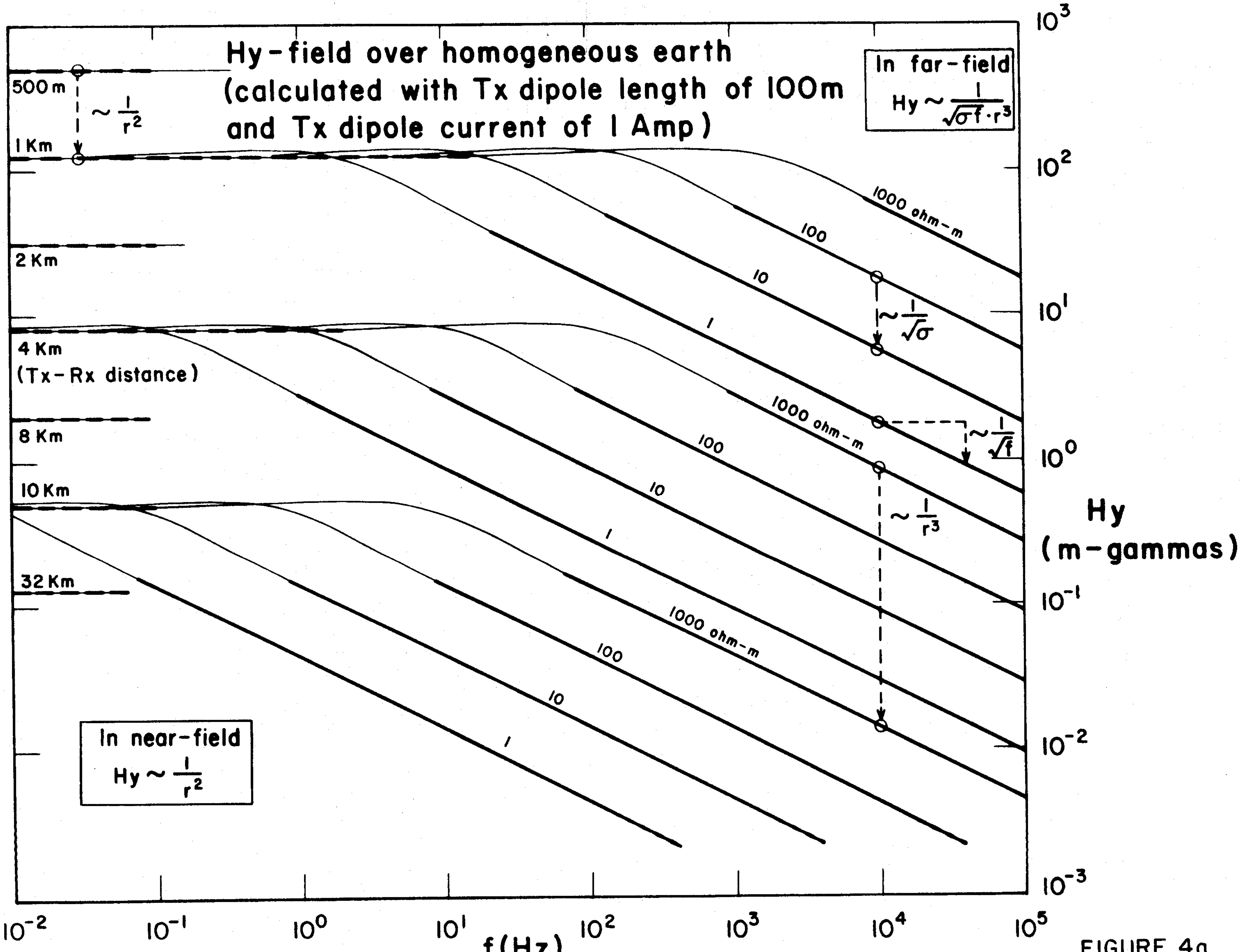
Hy-field over homogeneous earth
(calculated with Tx dipole length of 100m
and Tx dipole current of 1 Amp)
In far-field
$Hy \sim \frac{1}{\sqrt{\sigma f} \cdot r^3}$
In near-field
$Hy \sim \frac{1}{r^2}$
500 m
1 Km
2 Km
4 Km
(Tx-Rx distance)
8 Km
10 Km
32 Km
$\sim \frac{1}{r^2}$
$\sim \frac{1}{\sqrt{\sigma}}$
$\sim \frac{1}{\sqrt{f}}$
$\sim \frac{1}{r^3}$
1000 ohm-m
100
10
1
Hy
(m-gammas)
f (Hz)
10^{-2}
10^{-1}
10^{0}
10^{1}
10^{2}
10^{3}
10^{4}
10^{5}
10^{-3}

FIGURE 4a

PROFILES FOR APPARENT RESISTIVITIES CALCULATED for UNIFORM EARTH EXAMPLES

(a) Apparent resistivity vs frequency calculated by Cagniard equation over homogeneous earth of 1000 ohm.

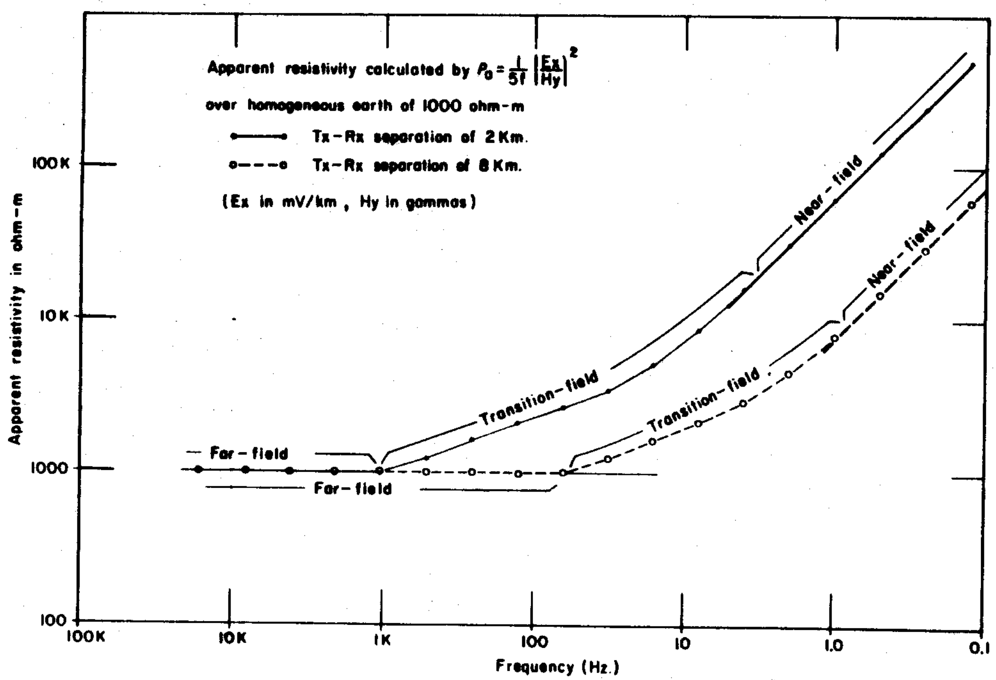

(b) Apparent resistivity vs frequency calculated using "near-field" equation over homogeneous earth of 1000 ohm.

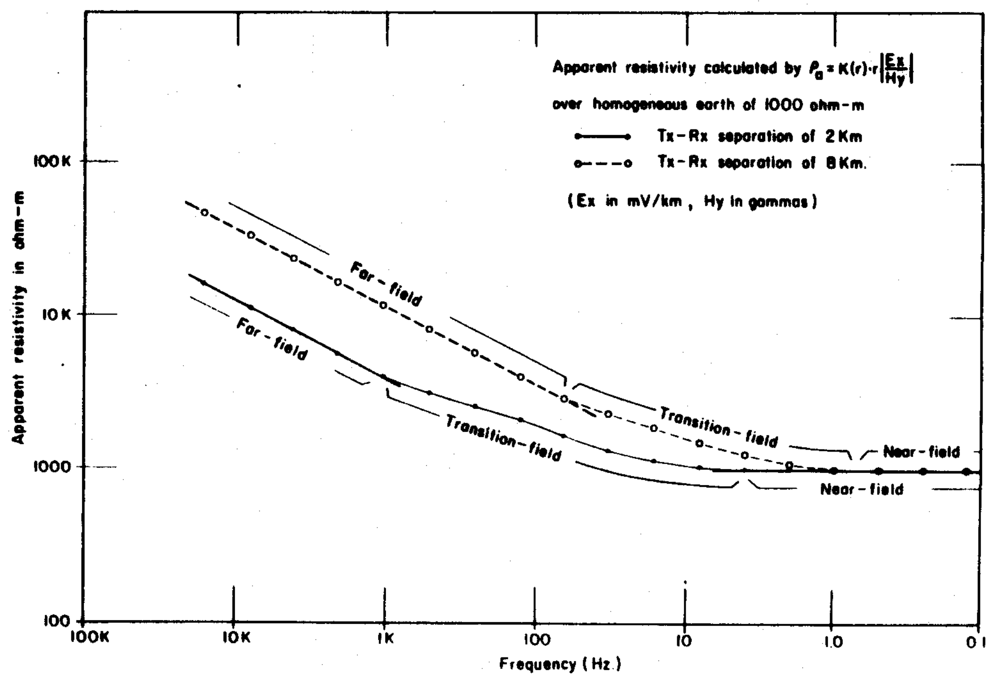

FIGURE 3

APPARENT RESISTIVITY PROFILES FROM FIELD DATA CAGNIARD (ρ_a) and "NEAR-FIELD" CORRECTED (ρ_a)

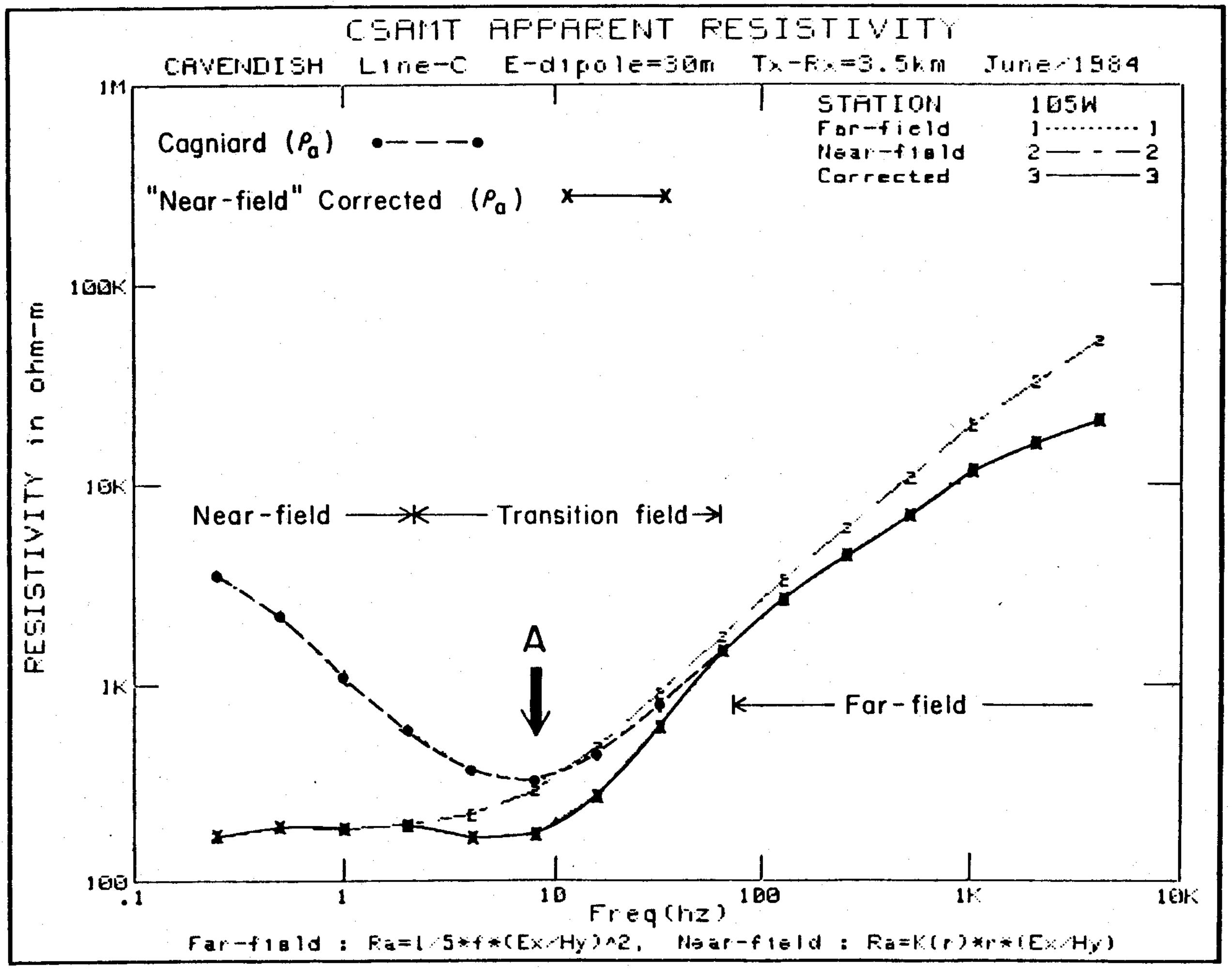

FIGURE 4c

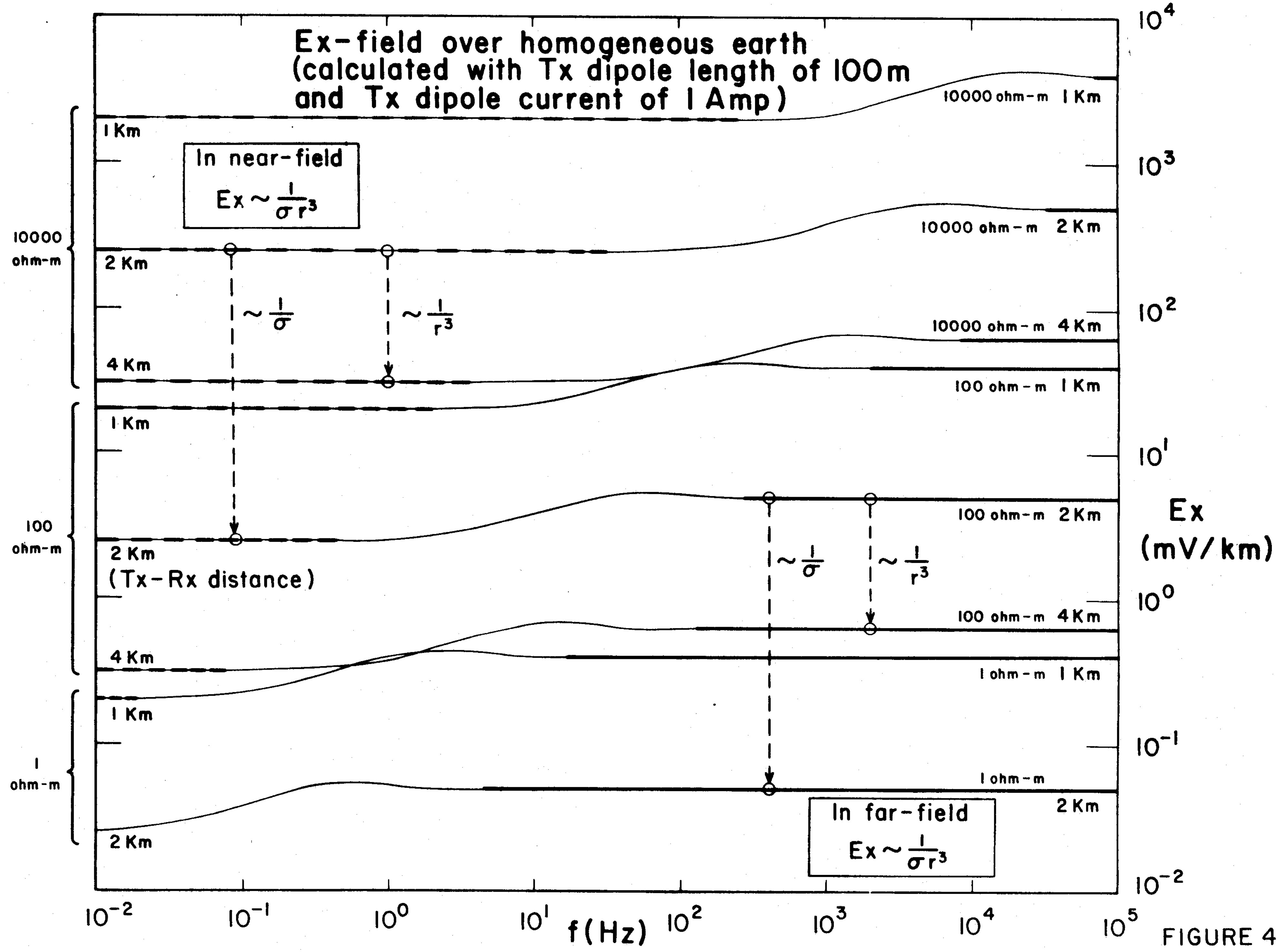

Ex-field over homogeneous earth
(calculated with Tx dipole length of 100m
and Tx dipole current of 1 Amp)
In near-field
Ex ~ 1/σr³
~ 1/σ
~ 1/r³
In far-field
Ex ~ 1/σr³
10000 ohm-m
100 ohm-m
1 ohm-m
1 Km
2 Km
4 Km
(Tx-Rx distance)
10000 ohm-m 1 Km
10000 ohm-m 2 Km
10000 ohm-m 4 Km
100 ohm-m 1 Km
100 ohm-m 2 Km
100 ohm-m 4 Km
1 ohm-m 1 Km
1 ohm-m 2 Km
Ex (mV/km)
f (Hz)

FIGURE 4b

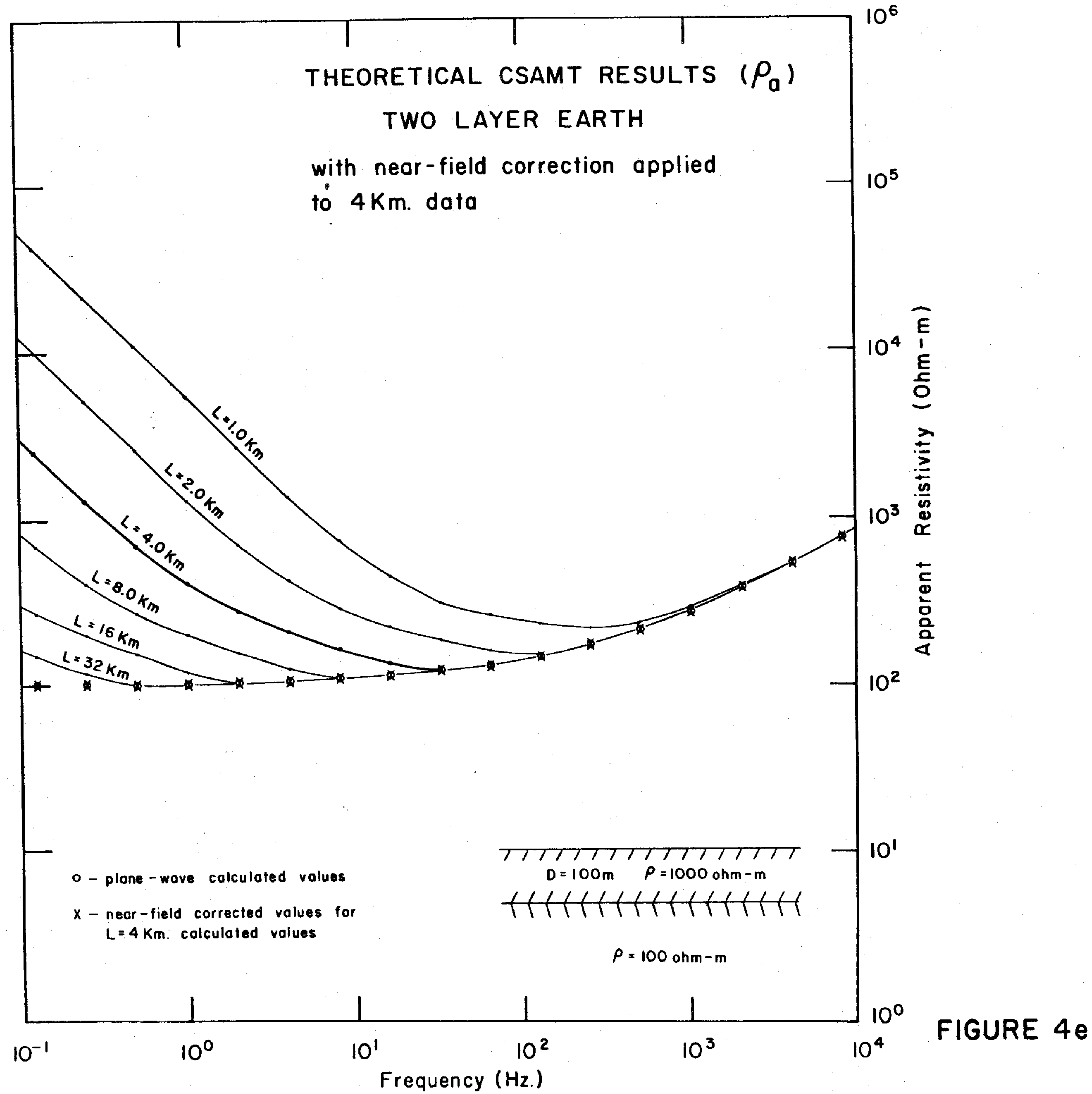

THEORETICAL CSAMT RESULTS (ρ_a)
TWO LAYER EARTH
with near-field correction applied
to 4 Km. data
L=1.0 Km
L=2.0 Km
L=4.0 Km
L=8.0 Km
L=16 Km
L=32 Km
o - plane-wave calculated values
X - near-field corrected values for
L=4 Km. calculated values
D=100m ρ=1000 ohm-m
ρ=100 ohm-m
Apparent Resistivity (Ohm-m)
Frequency (Hz.)
10^{-1}
10^{0}
10^{1}
10^{2}
10^{3}
10^{4}
10^{6}
10^{5}
10^{4}
10^{3}
10^{2}
10^{1}
10^{0}

FIGURE 4e

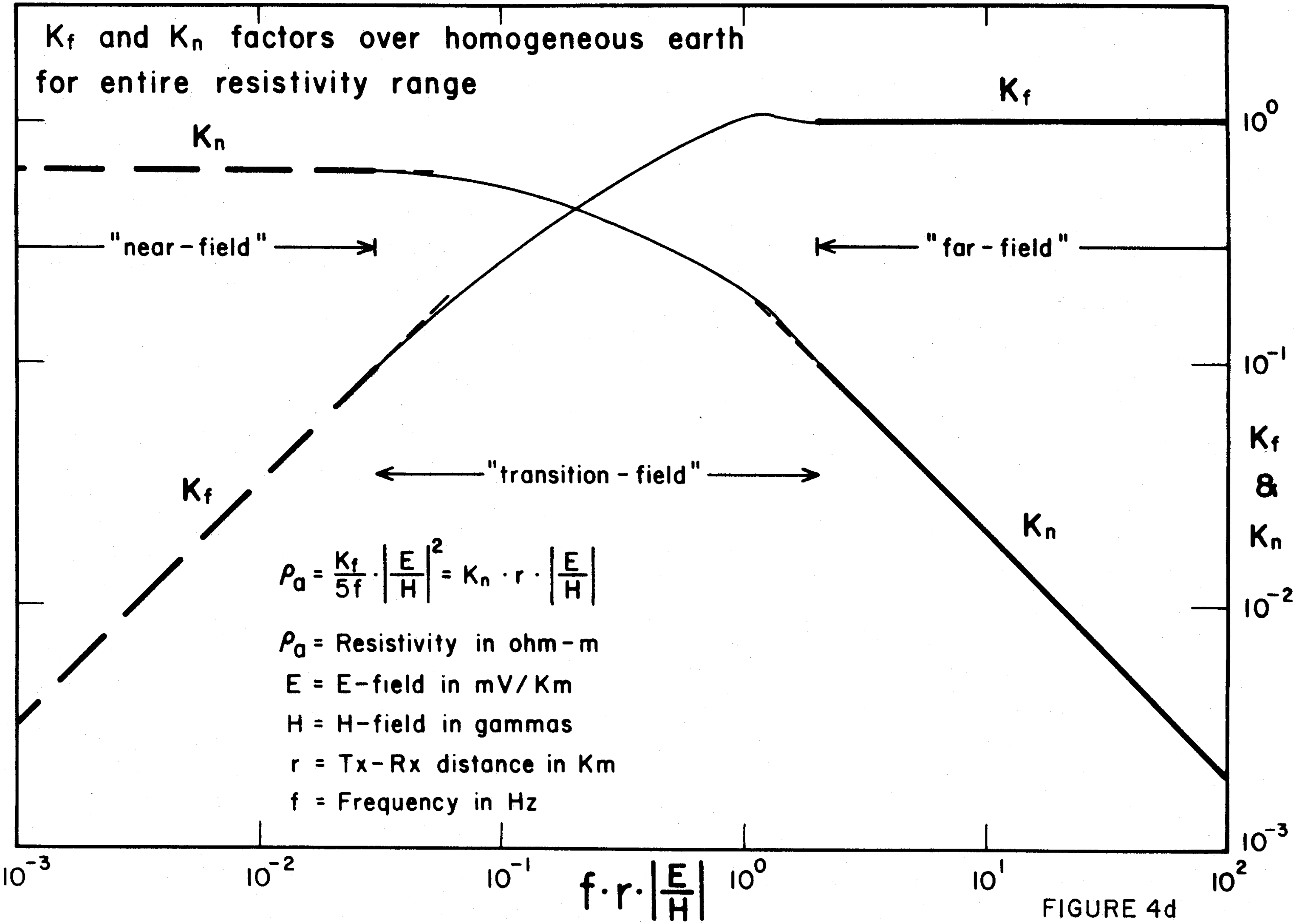

Kf and Kn factors over homogeneous earth
for entire resistivity range
Kf
Kn
"near-field"
"far-field"
"transition-field"
Kf
Kn
$\rho_a = \frac{K_f}{5f} \cdot \left|\frac{E}{H}\right|^2 = K_n \cdot r \cdot \left|\frac{E}{H}\right|$
ρ_a = Resistivity in ohm-m
E = E-field in mV/Km
H = H-field in gammas
r = Tx-Rx distance in Km
f = Frequency in Hz
10^0
10^{-1}
10^{-2}
10^{-3}
Kf & Kn
10^{-3}
10^{-2}
10^{-1}
10^0
10^1
10^2
$f \cdot r \cdot \left|\frac{E}{H}\right|$

FIGURE 4d

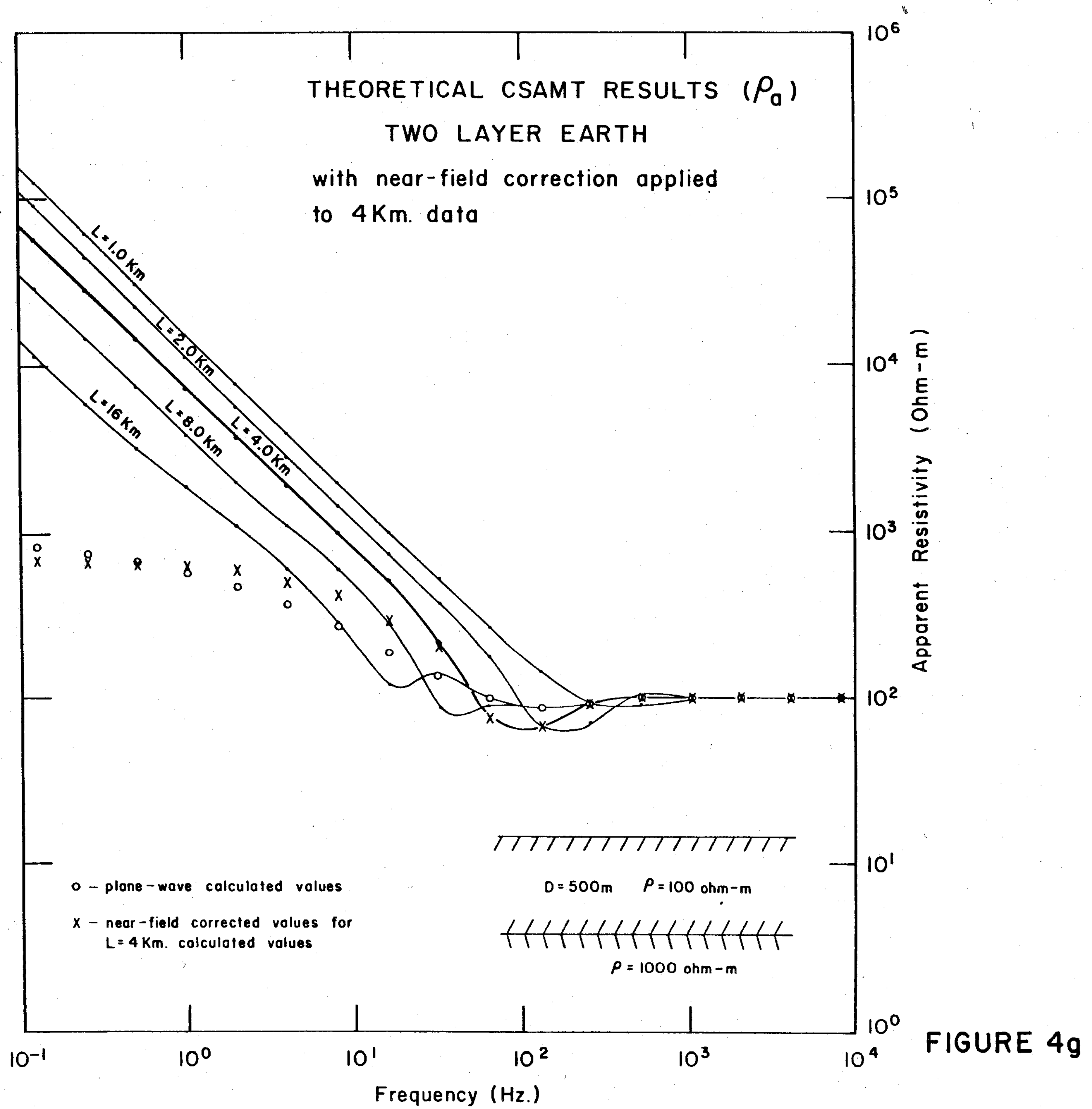
THEORETICAL CSAMT RESULTS (ρ_a)
TWO LAYER EARTH
with near-field correction applied
to 4 Km. data
L=1.0 Km
L=2.0 Km
L=4.0 Km
L=8.0 Km
L=16 Km
o – plane-wave calculated values
X – near-field corrected values for
L = 4 Km. calculated values
D = 500m
ρ = 100 ohm-m
ρ = 1000 ohm-m
10⁰
10¹
10²
10³
10⁴
10⁵
10⁶
10⁻¹
Apparent Resistivity (Ohm-m)
Frequency (Hz.)

FIGURE 4g

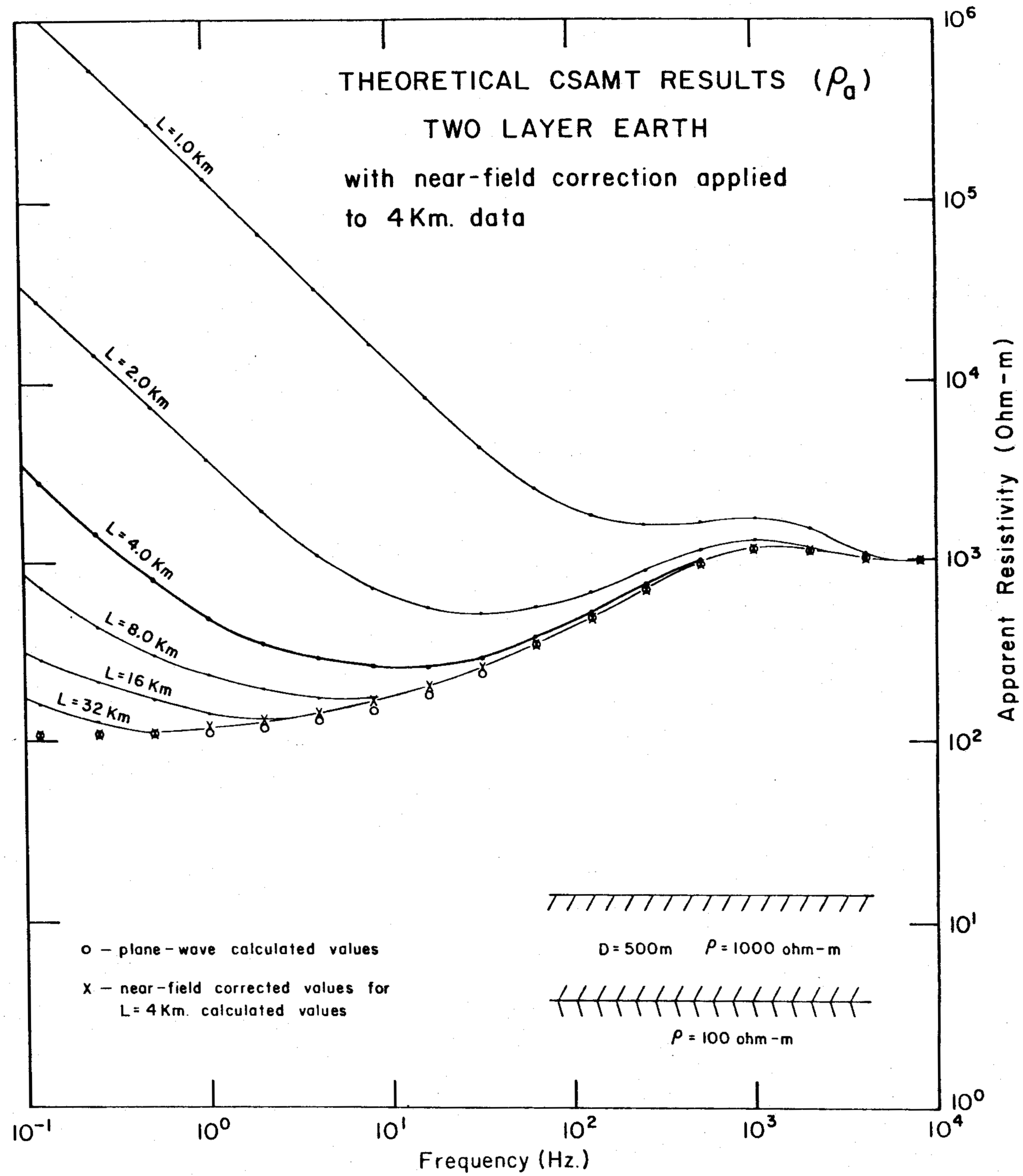

THEORETICAL CSAMT RESULTS (ρ_a)
TWO LAYER EARTH
with near-field correction applied
to 4 Km. data
L=1.0 Km
L=2.0 Km
L=4.0 Km
L=8.0 Km
L=16 Km
L=32 Km
o – plane-wave calculated values
X – near-field corrected values for
L=4 Km. calculated values
D=500m
ρ=1000 ohm-m
ρ=100 ohm-m
10^{-1}
10^{0}
10^{1}
10^{2}
10^{3}
10^{4}
Frequency (Hz.)
10^{6}
10^{5}
10^{4}
10^{3}
10^{2}
10^{1}
10^{0}
Apparent Resistivity (Ohm-m)

FIGURE 4f

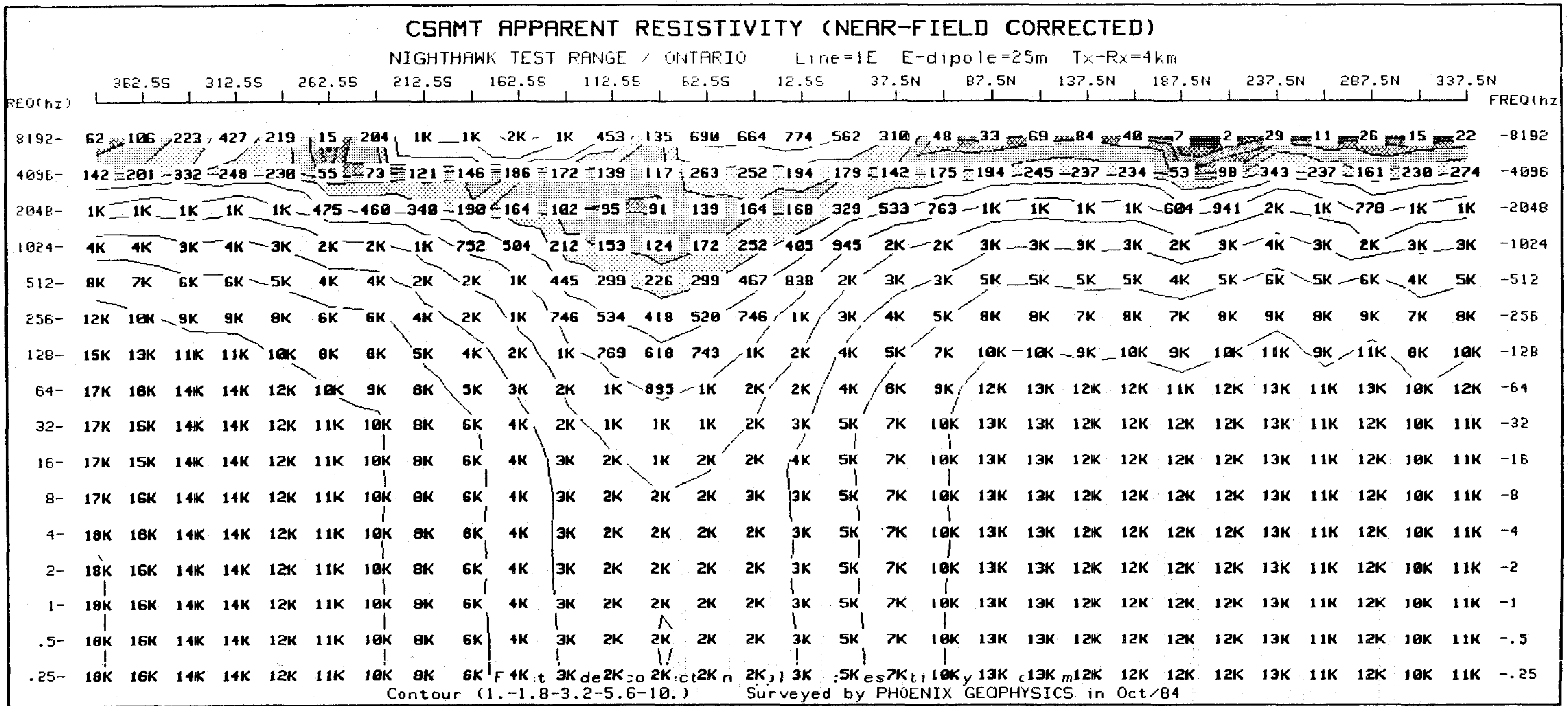
CSAMT APPARENT RESISTIVITY (NEAR-FIELD CORRECTED)
NIGHTHAWK TEST RANGE / ONTARIO   Line=1E E-dipole=25m Tx-Rx=4km
362.5S 312.5S 262.5S 212.5S 162.5S 112.5S 62.5S 12.5S 37.5N 87.5N 137.5N 187.5N 237.5N 287.5N 337.5N
FREQ(hz)
8192- 4096- 2048- 1024- 512- 256- 128- 64- 32- 16- 8- 4- 2- 1- .5- .25-
Contour (1.-1.8-3.2-5.6-10.)
Surveyed by PHOENIX GEOPHYSICS in Oct/84

FIGURE 5b

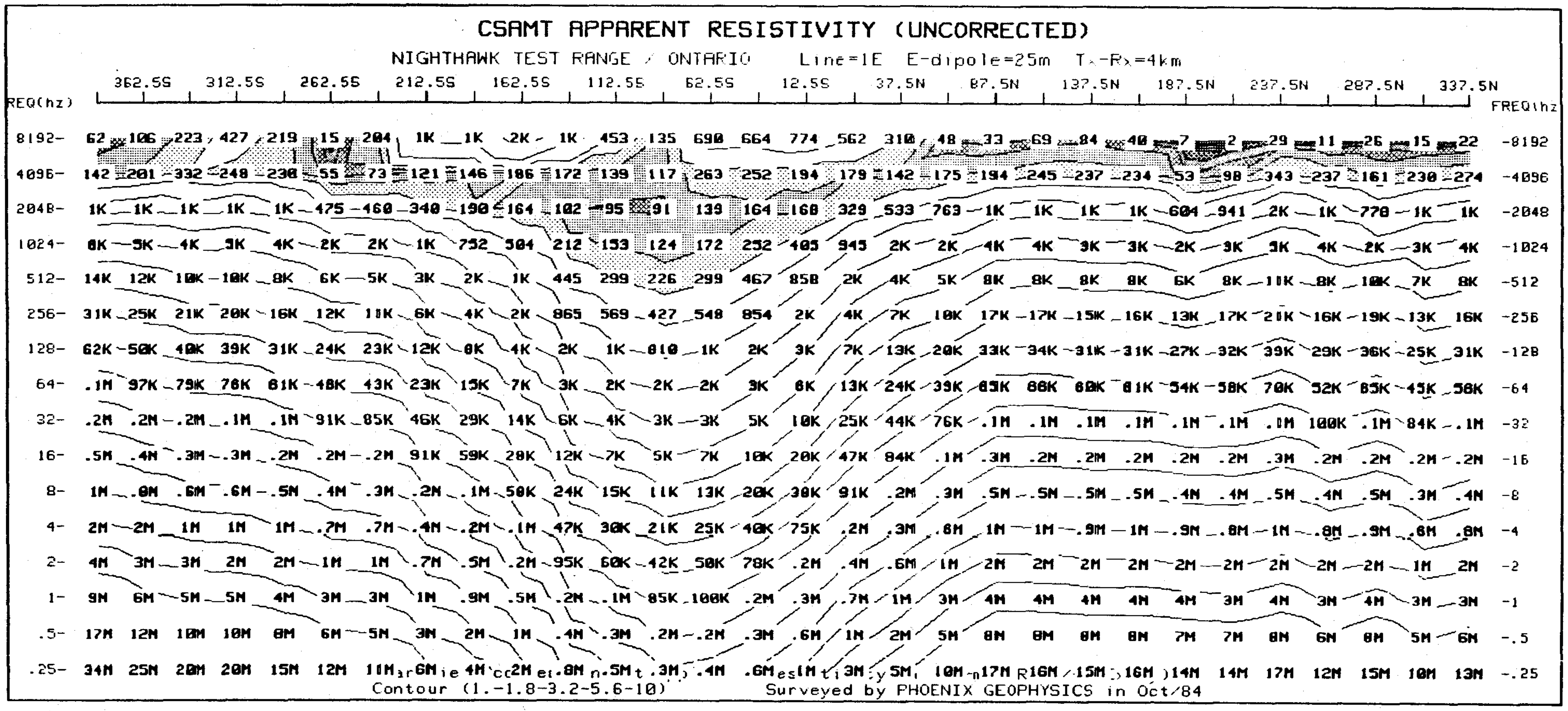
CSAMT APPARENT RESISTIVITY (UNCORRECTED)
NIGHTHAWK TEST RANGE / ONTARIO Line=1E E-dipole=25m Tx-Rx=4km
362.5S 312.5S 262.5S 212.5S 162.5S 112.5S 62.5S 12.5S 37.5N 87.5N 137.5N 187.5N 237.5N 287.5N 337.5N
FREQ(hz)
8192- 62 106 223 427 219 15 204 1K 1K 2K 1K 453 135 690 664 774 562 310 48 33 69 84 40 7 2 29 11 26 15 22 -8192
4096- 142 201 332 248 230 55 73 121 146 186 172 139 117 263 252 194 179 142 175 194 245 237 234 53 98 343 237 161 230 274 -4096
2048- 1K 1K 1K 1K 1K 475 460 340 190 164 102 95 91 139 164 168 329 533 763 1K 1K 1K 1K 604 941 2K 1K 770 1K 1K -2048
1024- 8K 5K 4K 3K 4K 2K 2K 1K 752 504 212 153 124 172 252 405 945 2K 2K 4K 4K 3K 3K 2K 3K 3K 4K 2K 3K 4K -1024
512- 14K 12K 10K 10K 8K 6K 5K 3K 2K 1K 445 299 226 299 467 858 2K 4K 5K 8K 8K 8K 8K 6K 8K 11K 8K 10K 7K 8K -512
256- 31K 25K 21K 20K 16K 12K 11K 6K 4K 2K 865 569 427 548 854 2K 4K 7K 10K 17K 17K 15K 16K 13K 17K 21K 16K 19K 13K 16K -256
128- 62K 50K 40K 39K 31K 24K 23K 12K 8K 4K 2K 1K 810 1K 2K 3K 7K 13K 20K 33K 34K 31K 31K 27K 32K 39K 29K 36K 25K 31K -128
64- .1M 97K 79K 76K 61K 48K 43K 23K 15K 7K 3K 2K 2K 2K 3K 6K 13K 24K 39K 65K 66K 60K 61K 54K 58K 70K 52K 65K 45K 58K -64
32- .2M .2M .2M .1M .1M 91K 85K 46K 29K 14K 6K 4K 3K 3K 5K 10K 25K 44K 76K .1M .1M .1M .1M .1M .1M .1M 100K .1M 84K .1M -32
16- .5M .4M .3M .3M .2M .2M .2M 91K 59K 28K 12K 7K 5K 7K 10K 20K 47K 84K .1M .3M .2M .2M .2M .2M .2M .3M .2M .2M .2M .2M -16
8- 1M .8M .6M .6M .5M .4M .3M .2M .1M 50K 24K 15K 11K 13K 20K 30K 91K .2M .3M .5M .5M .5M .5M .4M .4M .5M .4M .5M .3M .4M -8
4- 2M 2M 1M 1M 1M .7M .7M .4M .2M .1M 47K 30K 21K 25K 40K 75K .2M .3M .6M 1M 1M .9M 1M .9M .8M 1M .8M .9M .6M .8M -4
2- 4M 3M 3M 2M 2M 1M 1M .7M .5M .2M 95K 60K 42K 50K 78K .2M .4M .6M 1M 2M 2M 2M 2M 2M 2M 2M 2M 2M 1M 2M -2
1- 9M 6M 5M 5M 4M 3M 3M 1M .9M .5M .2M .1M 85K 100K .2M .3M .7M 1M 3M 4M 4M 4M 4M 4M 3M 4M 3M 4M 3M 3M -1
.5- 17M 12M 10M 10M 8M 6M 5M 3M 2M 1M .4M .3M .2M .2M .3M .6M 1M 2M 5M 8M 8M 8M 8M 7M 7M 8M 6M 8M 5M 6M -.5
.25- 34M 25M 20M 20M 15M 12M 11M 6M 4M 2M .8M .5M .3M .4M .6M 1M 3M 5M 10M 17M 16M 15M 16M 14M 14M 17M 12M 15M 10M 13M -.25
Contour (1.-1.8-3.2-5.6-10)
Surveyed by PHOENIX GEOPHYSICS in Oct/84

FIGURE 5a

SCALAR AMT APPARENT RESISTIVITY RESULTS

NIGHTHAWK LAKE GRID **LINE - 1E**

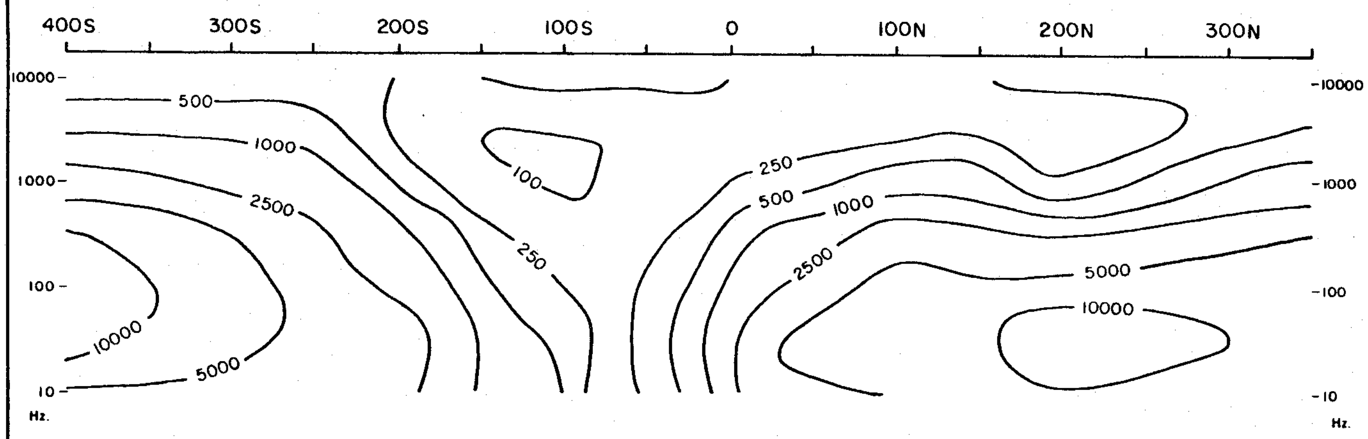

taken from Strangway et al (1982-83)

FIGURE 5c

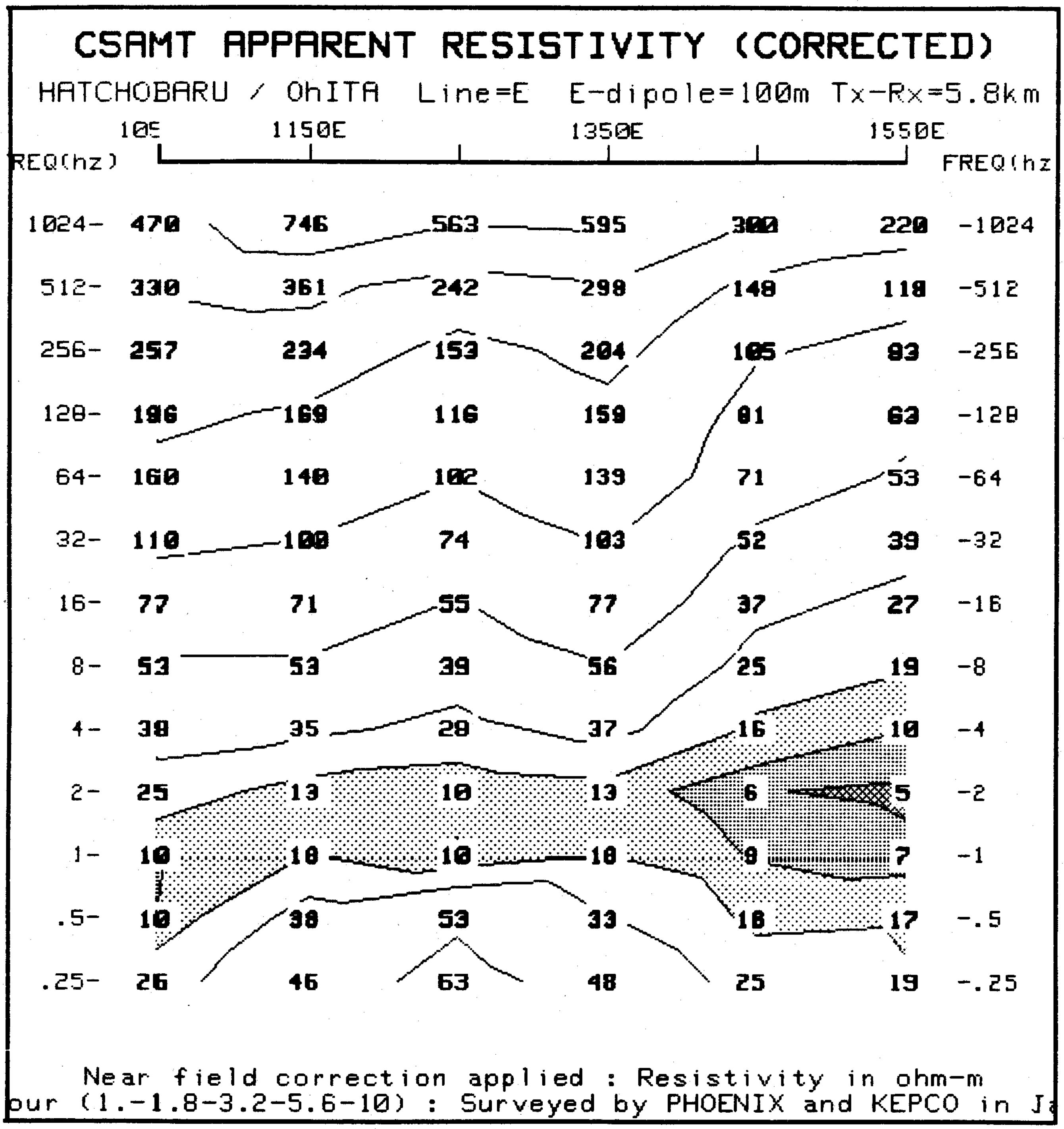

CSAMT APPARENT RESISTIVITY (CORRECTED)
HATCHOBARU / OhITA Line=E E-dipole=100m Tx-Rx=5.8km
105 1150E 1350E 1550E
REQ(hz) FREQ(hz
1024- 470 746 563 595 300 220 -1024
512- 330 361 242 298 148 118 -512
256- 257 234 153 204 105 83 -256
128- 196 169 116 159 81 63 -128
64- 160 140 102 139 71 53 -64
32- 110 100 74 103 52 39 -32
16- 77 71 55 77 37 27 -16
8- 53 53 39 56 25 19 -8
4- 38 35 28 37 16 10 -4
2- 25 13 10 13 6 5 -2
1- 10 10 10 10 9 7 -1
.5- 10 38 53 33 18 17 -.5
.25- 26 46 63 48 25 19 -.25
Near field correction applied : Resistivity in ohm-m
our (1.-1.8-3.2-5.6-10) : Surveyed by PHOENIX and KEPCO in J

FIGURE 6a

TRUE RESISTIVITY SECTION INTERPRETED
from CORRECTED CSAMT APPARENT RESISTIVITIES

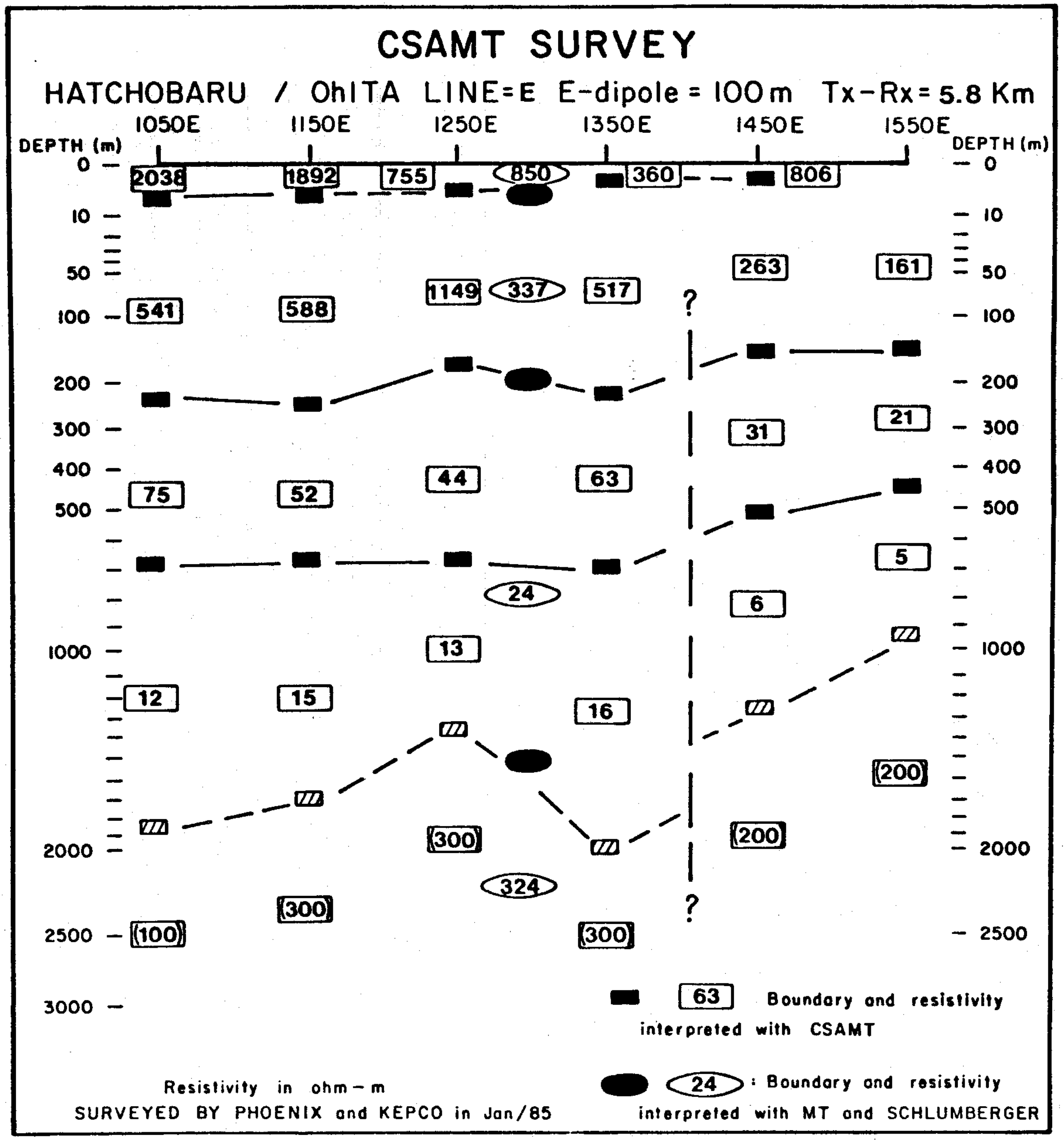

FIGURE 6b

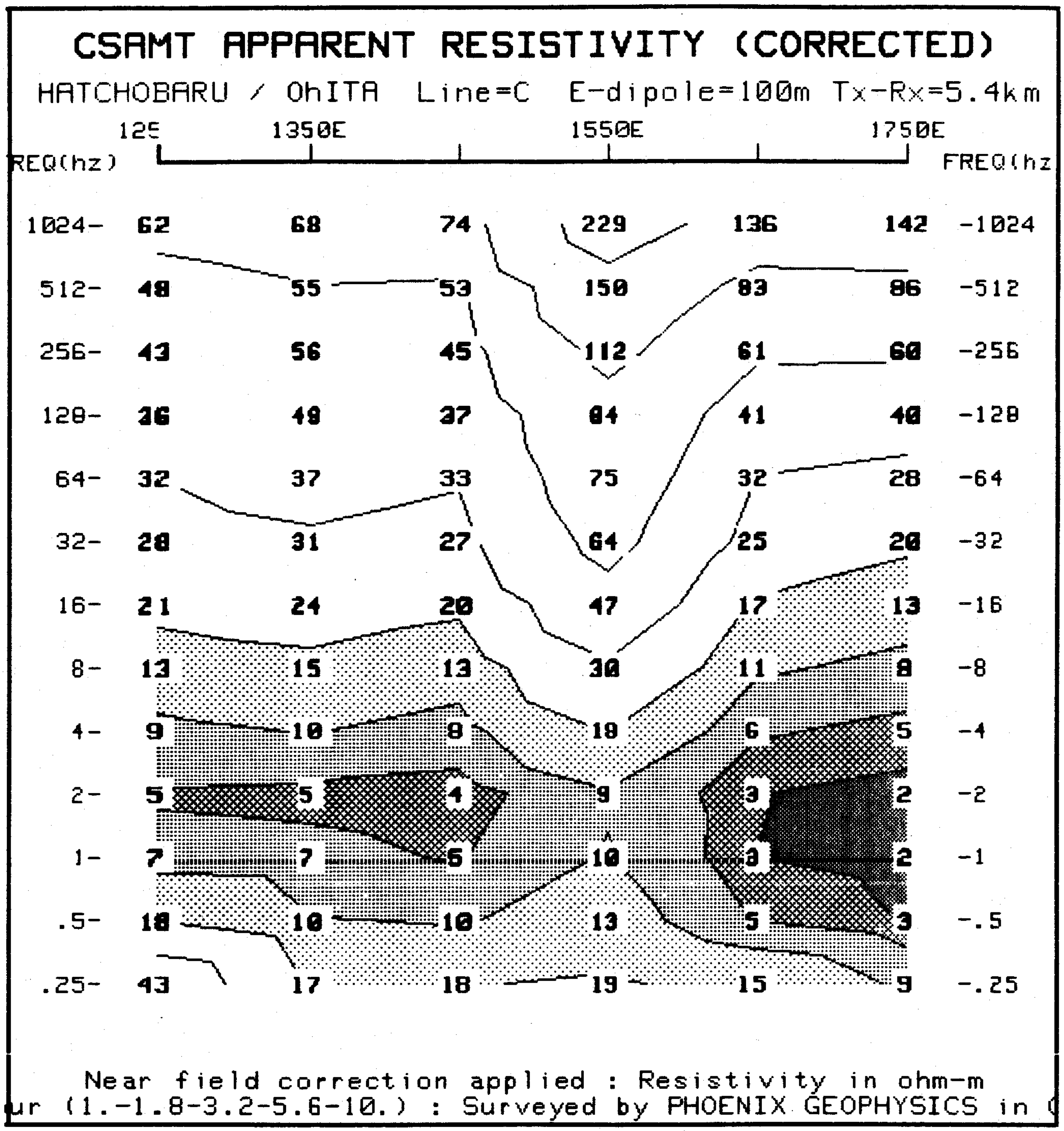

CSAMT APPARENT RESISTIVITY (CORRECTED)
HATCHOBARU / OhITA Line=C E-dipole=100m Tx-Rx=5.4km
125
1350E
1550E
1750E
REQ(hz)
FREQ(hz
1024- 62 68 74 229 136 142 -1024
512- 48 55 53 150 83 86 -512
256- 43 56 45 112 61 60 -256
128- 36 49 37 84 41 40 -128
64- 32 37 33 75 32 28 -64
32- 28 31 27 64 25 20 -32
16- 21 24 20 47 17 13 -16
8- 13 15 13 30 11 8 -8
4- 9 10 8 19 6 5 -4
2- 5 5 4 9 3 2 -2
1- 7 7 6 10 3 2 -1
.5- 18 10 10 13 5 3 -.5
.25- 43 17 18 19 15 9 -.25
Near field correction applied : Resistivity in ohm-m
ur (1.-1.8-3.2-5.6-10.) : Surveyed by PHOENIX GEOPHYSICS in

FIGURE 7a

TRUE RESISTIVITY SECTION INTERPRETED
from CORRECTED CSAMT APPARENT RESISTIVITIES

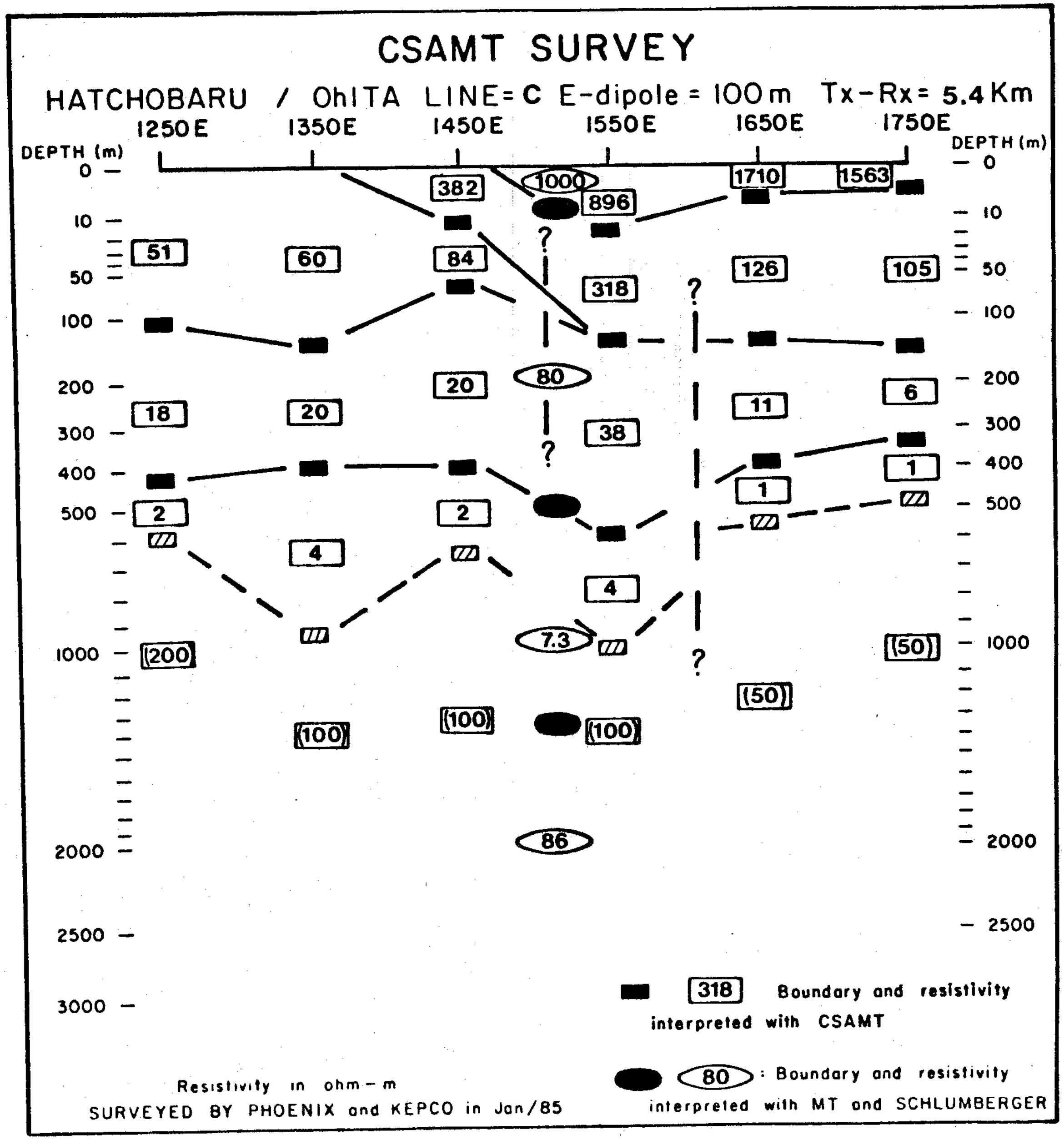

FIGURE 7b

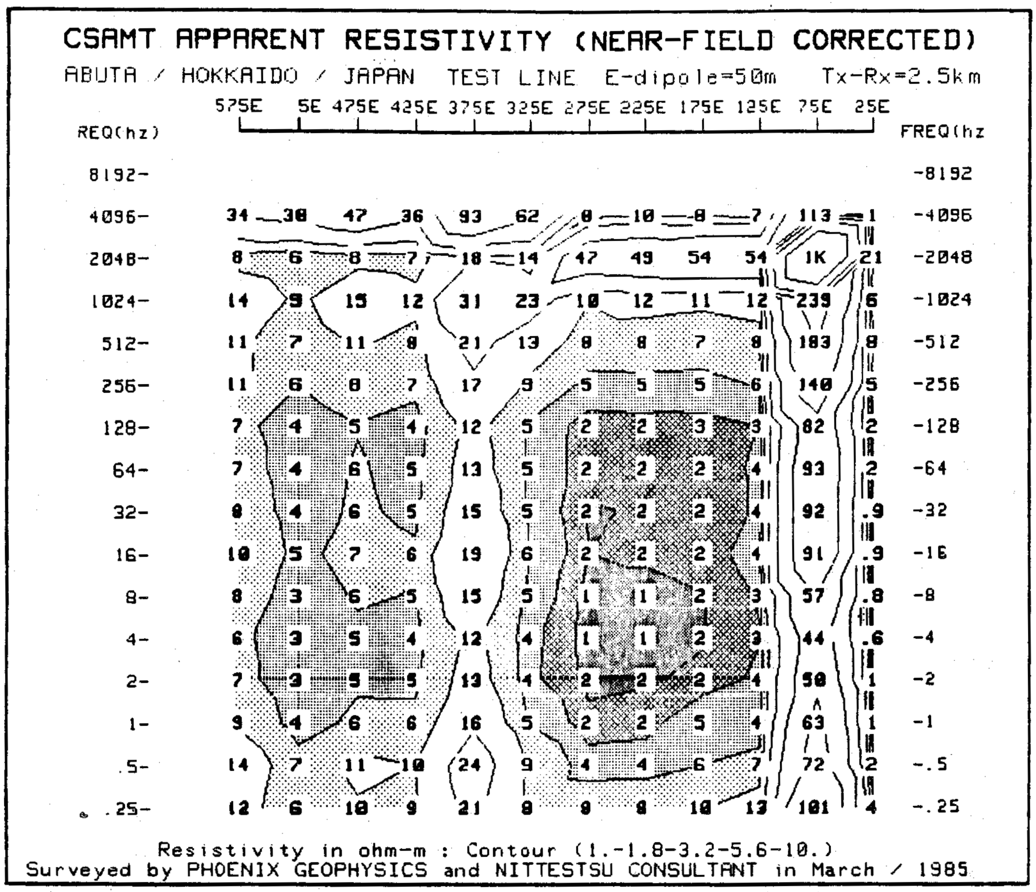

CSAMT APPARENT RESISTIVITY (NEAR-FIELD CORRECTED)
ABUTA / HOKKAIDO / JAPAN TEST LINE E-dipole=50m Tx-Rx=2.5km
575E 5E 475E 425E 375E 325E 275E 225E 175E 125E 75E 25E
REQ(hz)
FREQ(hz
8192- 4096- 2048- 1024- 512- 256- 128- 64- 32- 16- 8- 4- 2- 1- .5- .25-
Resistivity in ohm-m : Contour (1.-1.8-3.2-5.6-10.)
Surveyed by PHOENIX GEOPHYSICS and NITTESTSU CONSULTANT in March / 1985

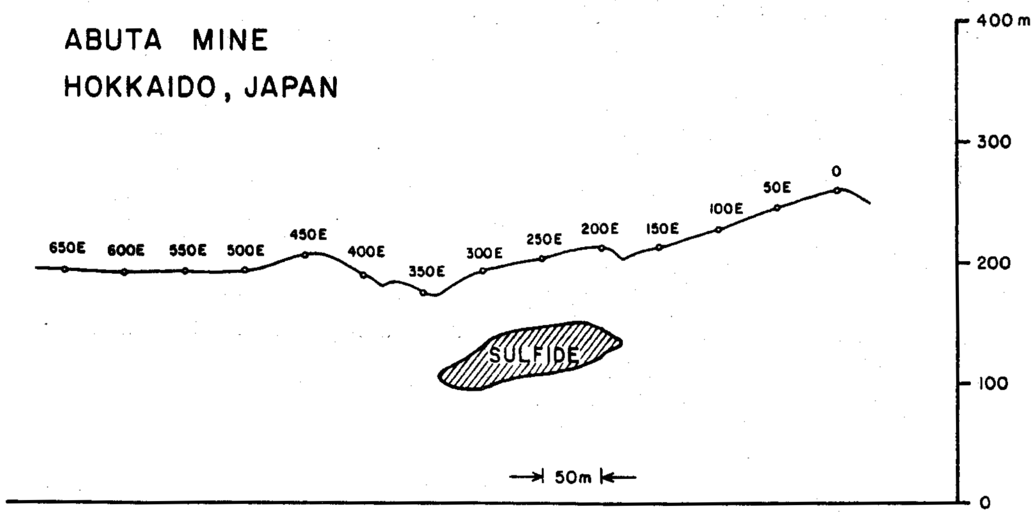

ABUTA MINE
HOKKAIDO, JAPAN
650E 600E 550E 500E 450E 400E 350E 300E 250E 200E 150E 100E 50E 0
SULFIDE
50m
400 m
300
200
100
0

FIGURE 8

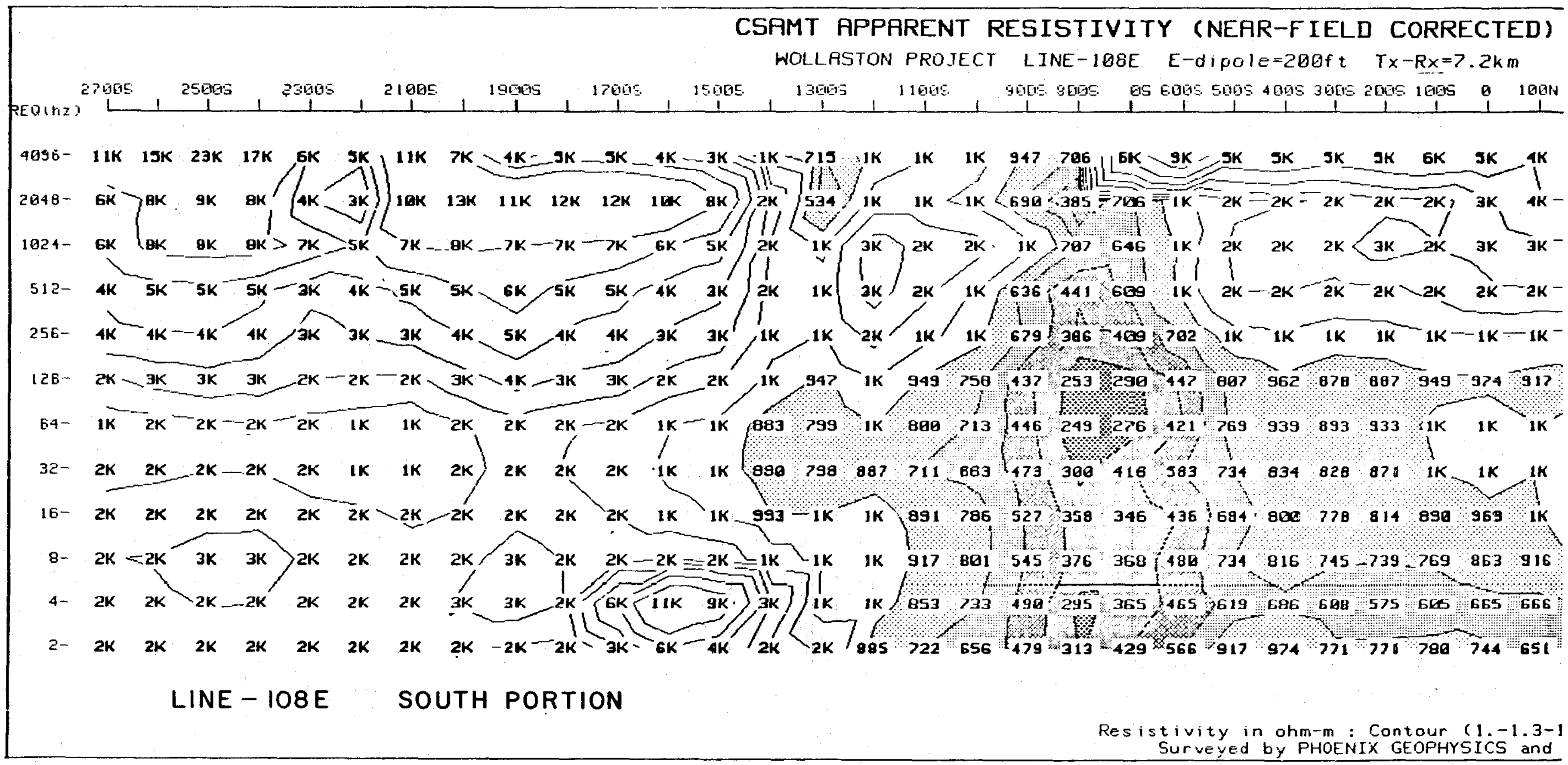
CSAMT APPARENT RESISTIVITY (NEAR-FIELD CORRECTED)
WOLLASTON PROJECT LINE-108E E-dipole=200ft Tx-Rx=7.2km
2700S 2500S 2300S 2100S 1900S 1700S 1500S 1300S 1100S 900S 800S 0S 600S 500S 400S 300S 200S 100S 0 100N
REQ(hz)
4096- 11K 15K 23K 17K 6K 5K 11K 7K 4K 5K 5K 4K 3K 1K 715 1K 1K 1K 947 706 6K 9K 5K 5K 5K 5K 6K 5K 4K
2048- 6K 8K 9K 8K 4K 3K 10K 13K 11K 12K 12K 10K 8K 2K 534 1K 1K 1K 690 385 706 1K 2K 2K 2K 2K 2K 3K 4K
1024- 6K 8K 8K 8K 7K 5K 7K 8K 7K 7K 7K 6K 5K 2K 1K 3K 2K 2K 1K 707 646 1K 2K 2K 2K 3K 2K 3K 3K
512- 4K 5K 5K 5K 3K 4K 5K 5K 6K 5K 5K 4K 3K 2K 1K 3K 2K 1K 636 441 609 1K 2K 2K 2K 2K 2K 2K 2K
256- 4K 4K 4K 4K 3K 3K 3K 4K 5K 4K 4K 3K 3K 1K 1K 2K 1K 1K 679 386 409 702 1K 1K 1K 1K 1K 1K 1K
128- 2K 3K 3K 3K 2K 2K 2K 3K 4K 3K 3K 2K 2K 1K 947 1K 949 750 437 253 290 447 807 962 878 887 949 974 917
64- 1K 2K 2K 2K 2K 1K 1K 2K 2K 2K 2K 1K 1K 883 799 1K 800 713 446 249 276 421 769 939 893 933 1K 1K 1K
32- 2K 2K 2K 2K 2K 1K 1K 2K 2K 2K 2K 1K 1K 880 798 887 711 663 473 300 416 583 734 834 828 871 1K 1K 1K
16- 2K 2K 2K 2K 2K 2K 2K 2K 2K 2K 2K 1K 1K 993 1K 1K 891 786 527 358 346 436 684 800 778 814 890 969 1K
8- 2K 2K 3K 3K 2K 2K 2K 2K 3K 2K 2K 2K 2K 1K 1K 1K 917 801 545 376 368 480 734 816 745 739 769 863 916
4- 2K 2K 2K 2K 2K 2K 2K 3K 3K 2K 6K 11K 9K 3K 1K 1K 853 733 490 295 365 465 619 686 608 575 665 665 666
2- 2K 2K 2K 2K 2K 2K 2K 2K 2K 2K 3K 6K 4K 2K 2K 885 722 656 479 313 429 566 917 974 771 771 780 744 651
LINE - 108E SOUTH PORTION
Resistivity in ohm-m : Contour (1.-1.3-1
Surveyed by PHOENIX GEOPHYSICS and

FIGURE 9a-S

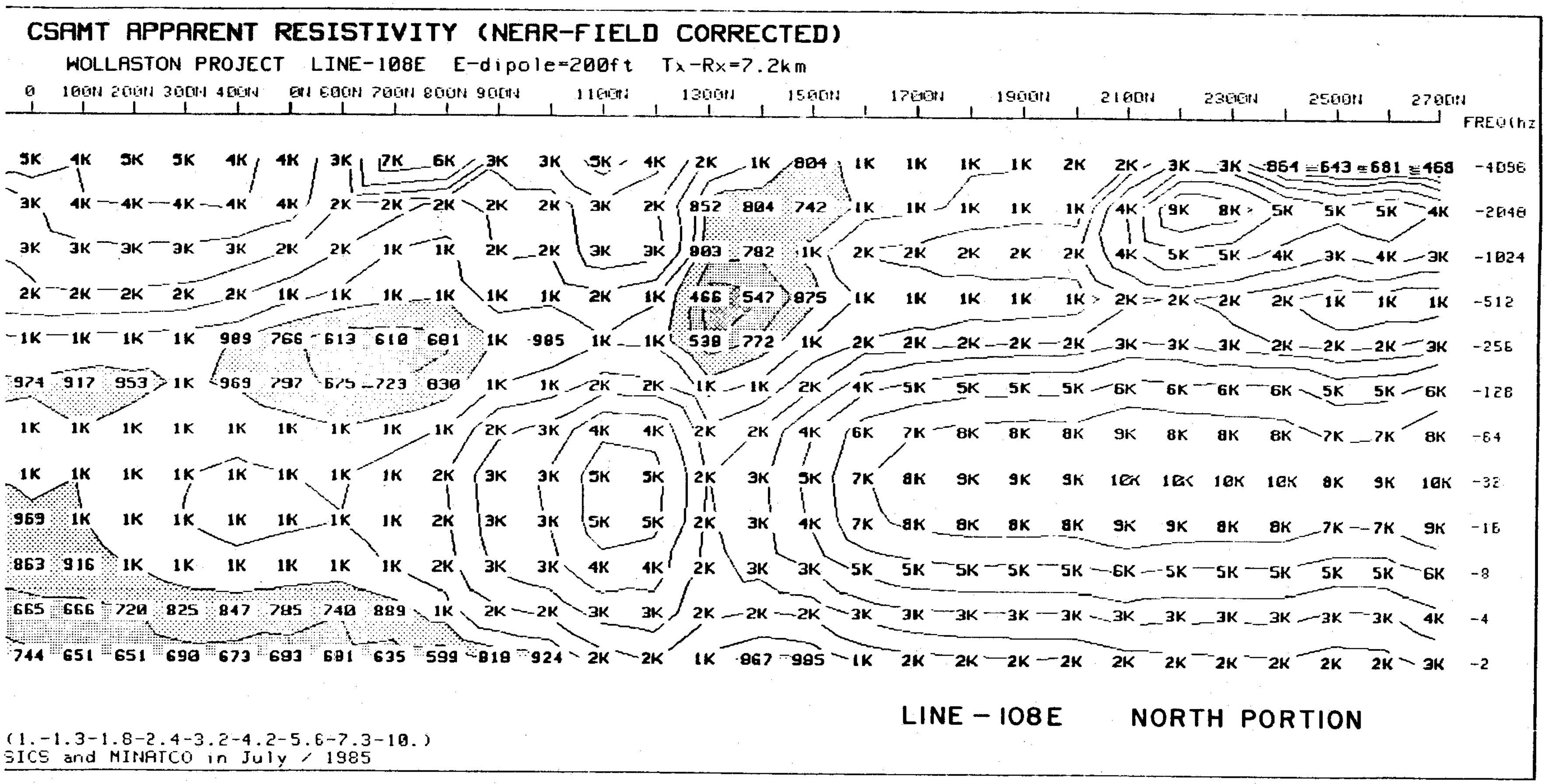
CSAMT APPARENT RESISTIVITY (NEAR-FIELD CORRECTED)
WOLLASTON PROJECT LINE-108E E-dipole=200ft Tx-Rx=7.2km
0 100N 200N 300N 400N 0N 600N 700N 800N 900N 1100N 1300N 1500N 1700N 1900N 2100N 2300N 2500N 2700N
FREQ(hz)
5K 4K 5K 5K 4K 4K 3K 7K 6K 3K 3K 5K 4K 2K 1K 804 1K 1K 1K 1K 2K 2K 3K 3K 864 643 681 468 -4096
3K 4K 4K 4K 4K 4K 2K 2K 2K 2K 2K 3K 2K 852 804 742 1K 1K 1K 1K 1K 4K 9K 8K 5K 5K 5K 4K -2048
3K 3K 3K 3K 3K 2K 2K 1K 1K 2K 2K 3K 3K 803 782 1K 2K 2K 2K 2K 2K 4K 5K 5K 4K 3K 4K 3K -1024
2K 2K 2K 2K 2K 1K 1K 1K 1K 1K 1K 2K 1K 466 547 875 1K 1K 1K 1K 1K 2K 2K 2K 2K 1K 1K 1K -512
1K 1K 1K 1K 989 766 613 610 681 1K 985 1K 1K 538 772 1K 2K 2K 2K 2K 2K 3K 3K 3K 2K 2K 2K 3K -256
974 917 953 1K 969 797 675 723 830 1K 1K 2K 2K 1K 1K 2K 4K 5K 5K 5K 5K 6K 6K 6K 6K 5K 5K 6K -128
1K 1K 1K 1K 1K 1K 1K 1K 1K 2K 3K 4K 4K 2K 2K 4K 6K 7K 8K 8K 8K 9K 8K 8K 8K 7K 7K 8K -64
1K 1K 1K 1K 1K 1K 1K 1K 2K 3K 3K 5K 5K 2K 3K 5K 7K 8K 9K 9K 9K 10K 10K 10K 10K 8K 9K 10K -32
969 1K 1K 1K 1K 1K 1K 1K 2K 3K 3K 5K 5K 2K 3K 4K 7K 8K 8K 8K 8K 9K 9K 8K 8K 7K 7K 9K -16
863 916 1K 1K 1K 1K 1K 1K 2K 3K 3K 4K 4K 2K 3K 3K 5K 5K 5K 5K 5K 6K 5K 5K 5K 5K 5K 6K -8
665 666 720 825 847 785 740 889 1K 2K 2K 3K 3K 2K 2K 2K 3K 3K 3K 3K 3K 3K 3K 3K 3K 3K 3K 4K -4
744 651 651 690 673 693 691 635 599 818 924 2K 2K 1K 867 985 1K 2K 2K 2K 2K 2K 2K 2K 2K 2K 2K 3K -2
LINE – 108E NORTH PORTION
(1.-1.3-1.8-2.4-3.2-4.2-5.6-7.3-10.)
SICS and MINATCO in July / 1985

FIGURE 9a-N

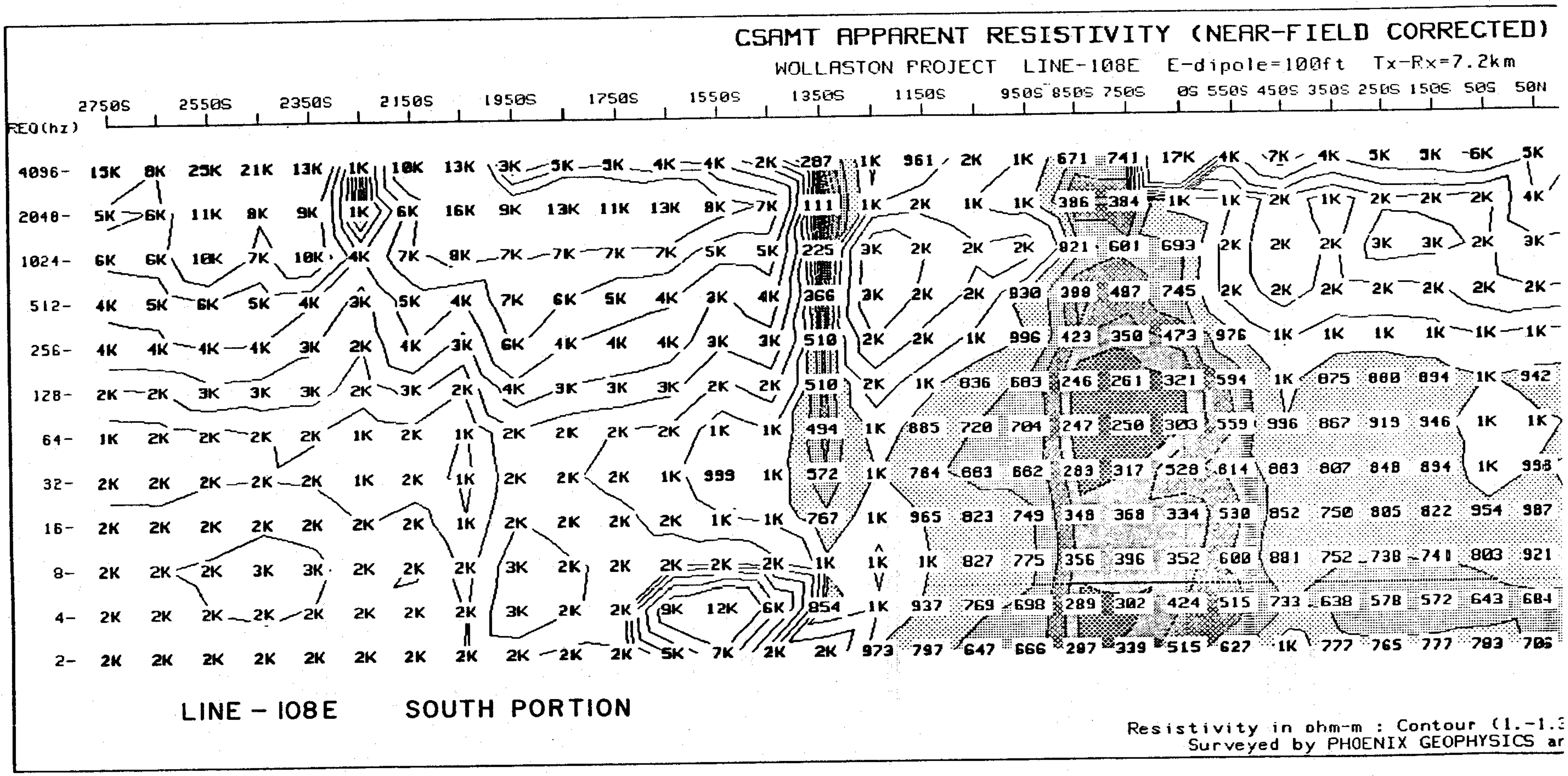

CSAMT APPARENT RESISTIVITY (NEAR-FIELD CORRECTED)
WOLLASTON PROJECT LINE-108E E-dipole=100ft Tx-Rx=7.2km
2750S 2550S 2350S 2150S 1950S 1750S 1550S 1350S 1150S 950S 850S 750S 0S 550S 450S 350S 250S 150S 50S 50N
REQ(hz)
4096- 2048- 1024- 512- 256- 128- 64- 32- 16- 8- 4- 2-
LINE - 108E SOUTH PORTION
Resistivity in ohm-m : Contour (1.-1.3
Surveyed by PHOENIX GEOPHYSICS ar

FIGURE 9b-S

CSAMT APPARENT RESISTIVITY (NEAR-FIELD CORRECTED)

WOLLASTON PROJECT LINE-108E E-dipole=100ft Tx-Rx=7.2km

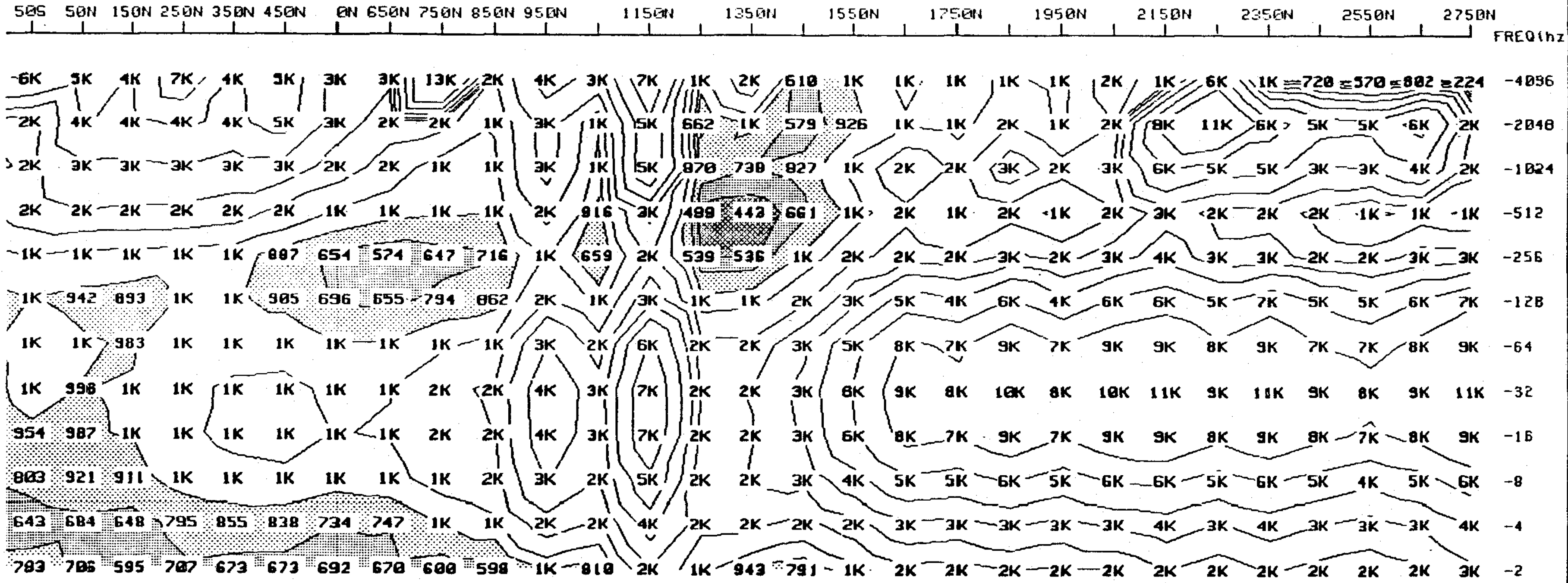

LINE - 108E NORTH PORTION

r (1.-1.3-1.8-2.4-3.2-4.2-5.6-7.3-10.)
HYSICS and MINATCO in July / 1985

FIGURE 9b-N

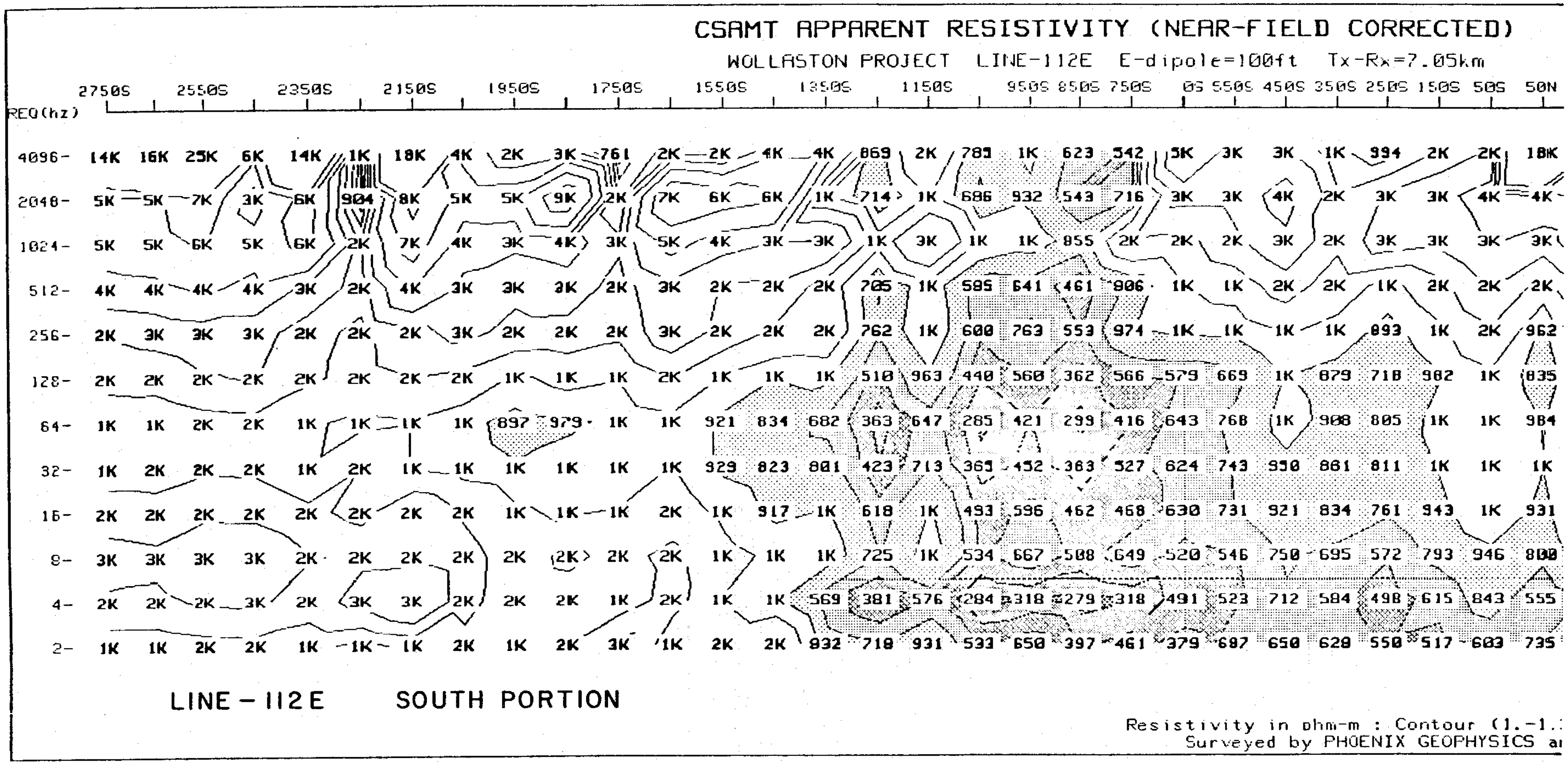
CSAMT APPARENT RESISTIVITY (NEAR-FIELD CORRECTED)
WOLLASTON PROJECT LINE-112E E-dipole=100ft Tx-Rx=7.05km
2750S 2550S 2350S 2150S 1950S 1750S 1550S 1350S 1150S 950S 850S 750S 0S 550S 450S 350S 250S 150S 50S 50N
REQ(hz)
4096- 2048- 1024- 512- 256- 128- 64- 32- 16- 8- 4- 2-
LINE - 112E SOUTH PORTION
Resistivity in ohm-m : Contour (1.-1.
Surveyed by PHOENIX GEOPHYSICS a

FIGURE 9c-S

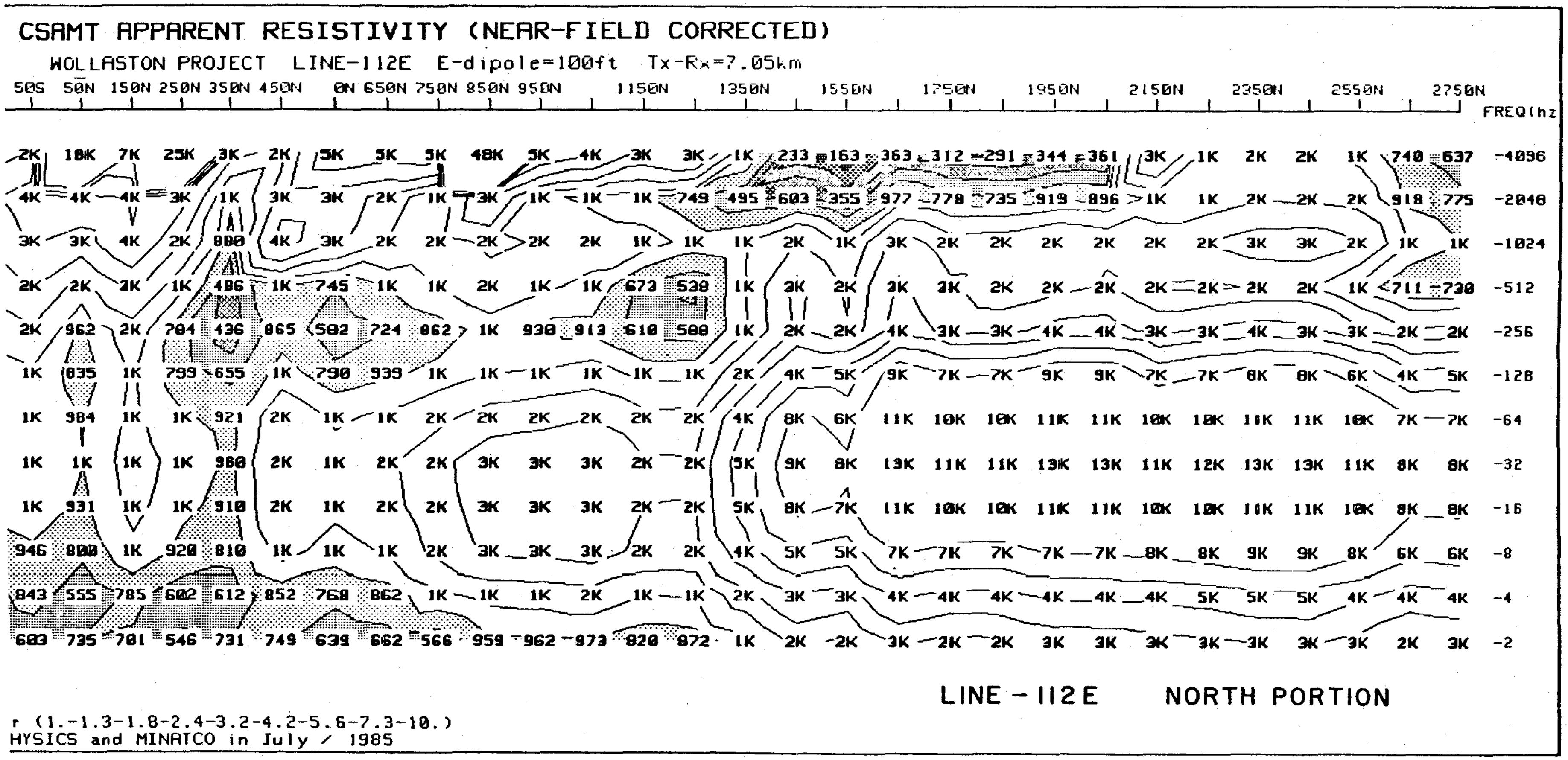
CSAMT APPARENT RESISTIVITY (NEAR-FIELD CORRECTED)
WOLLASTON PROJECT LINE-112E E-dipole=100ft Tx-Rx=7.05km
50S 50N 150N 250N 350N 450N 0N 650N 750N 850N 950N 1150N 1350N 1550N 1750N 1950N 2150N 2350N 2550N 2750N
FREQ(hz
2K 18K 7K 25K 3K 2K 5K 5K 5K 48K 5K 4K 3K 3K 1K 233 163 363 312 291 344 361 3K 1K 2K 2K 1K 740 637 -4096
4K 4K 4K 3K 1K 3K 3K 2K 1K 3K 1K 1K 1K 749 495 603 355 977 778 735 919 896 1K 1K 2K 2K 2K 918 775 -2048
3K 3K 4K 2K 888 4K 3K 2K 2K 2K 2K 2K 1K 1K 1K 2K 1K 3K 2K 2K 2K 2K 2K 2K 3K 3K 2K 1K 1K -1024
2K 2K 3K 1K 486 1K 745 1K 1K 2K 1K 1K 673 538 1K 3K 2K 3K 3K 2K 2K 2K 2K 2K 2K 2K 1K 711 730 -512
2K 962 2K 704 436 865 582 724 862 1K 930 913 610 580 1K 2K 2K 4K 3K 3K 4K 4K 3K 3K 4K 3K 3K 2K 2K -256
1K 835 1K 799 655 1K 790 939 1K 1K 1K 1K 1K 1K 2K 4K 5K 9K 7K 7K 9K 9K 7K 7K 8K 8K 6K 4K 5K -128
1K 984 1K 1K 921 2K 1K 1K 2K 2K 2K 2K 2K 2K 4K 8K 6K 11K 10K 10K 11K 11K 10K 10K 11K 11K 10K 7K 7K -64
1K 1K 1K 1K 980 2K 1K 2K 2K 3K 3K 3K 2K 2K 5K 9K 8K 13K 11K 11K 13K 13K 11K 12K 13K 13K 11K 8K 8K -32
1K 931 1K 1K 910 2K 1K 2K 2K 3K 3K 3K 2K 2K 5K 8K 7K 11K 10K 10K 11K 11K 10K 10K 11K 11K 10K 8K 8K -16
946 888 1K 920 810 1K 1K 1K 2K 3K 3K 3K 2K 2K 4K 5K 5K 7K 7K 7K 7K 7K 8K 8K 9K 9K 8K 6K 6K -8
843 555 785 602 612 852 768 862 1K 1K 1K 2K 1K 1K 2K 3K 3K 4K 4K 4K 4K 4K 4K 5K 5K 5K 4K 4K 4K -4
683 735 701 546 731 749 639 662 566 959 962 973 820 872 1K 2K 2K 3K 2K 2K 3K 3K 3K 3K 3K 3K 3K 2K 3K -2
LINE - 112E NORTH PORTION
r (1.-1.3-1.8-2.4-3.2-4.2-5.6-7.3-10.)
HYSICS and MINATCO in July / 1985

FIGURE 9c-N

NORTH-SOUTH TRUE SCALE STRUCTURAL CROSS-SECTION
COREY EAST PINNACLE REEF ENNISKILLEN TWP.

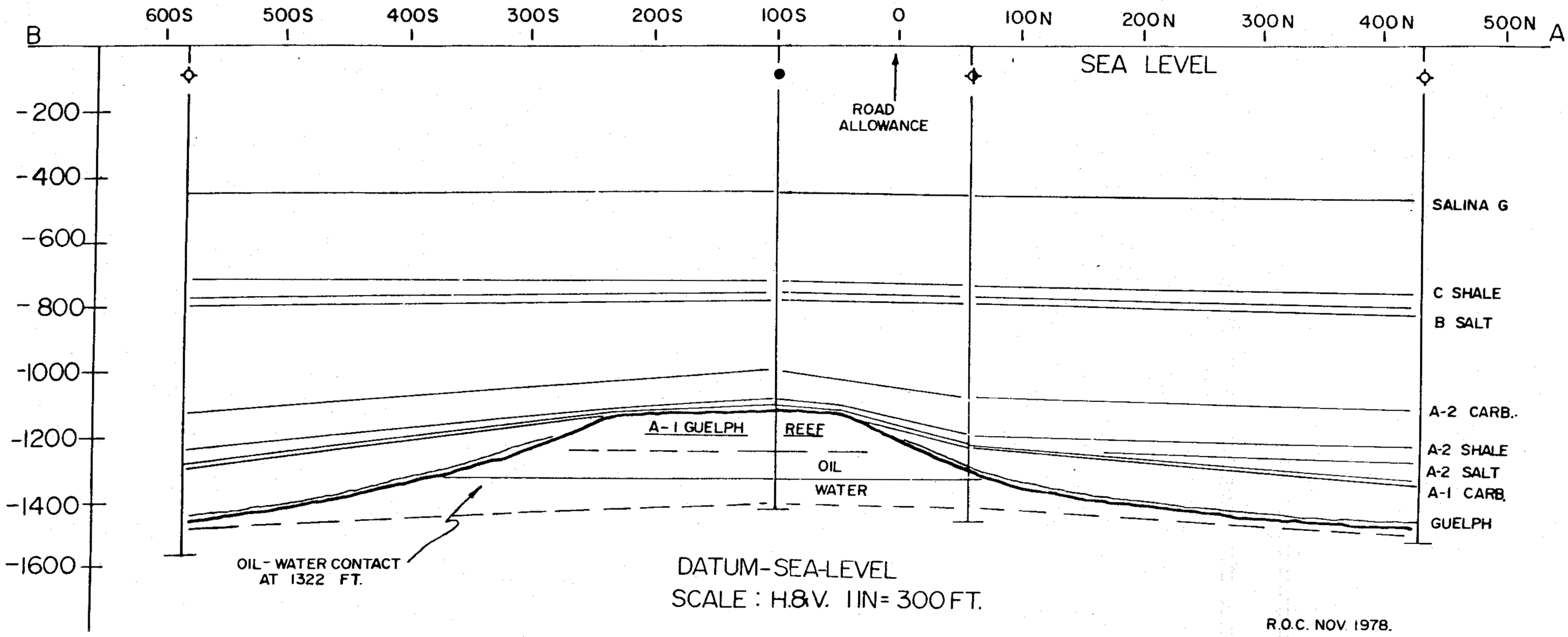

FIGURE 10a

PHOENIX GEOPHYSICS
2D FINITE ELEMENT
CSAMT MODELING

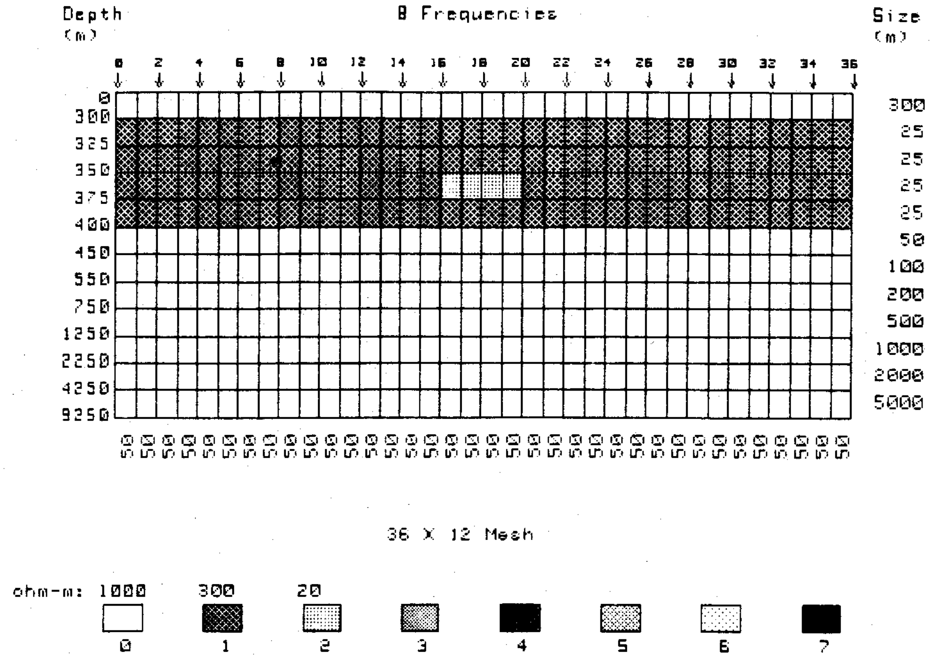

Execution Time = 609 sec on HP9000-520 (one CPU) desktop computer

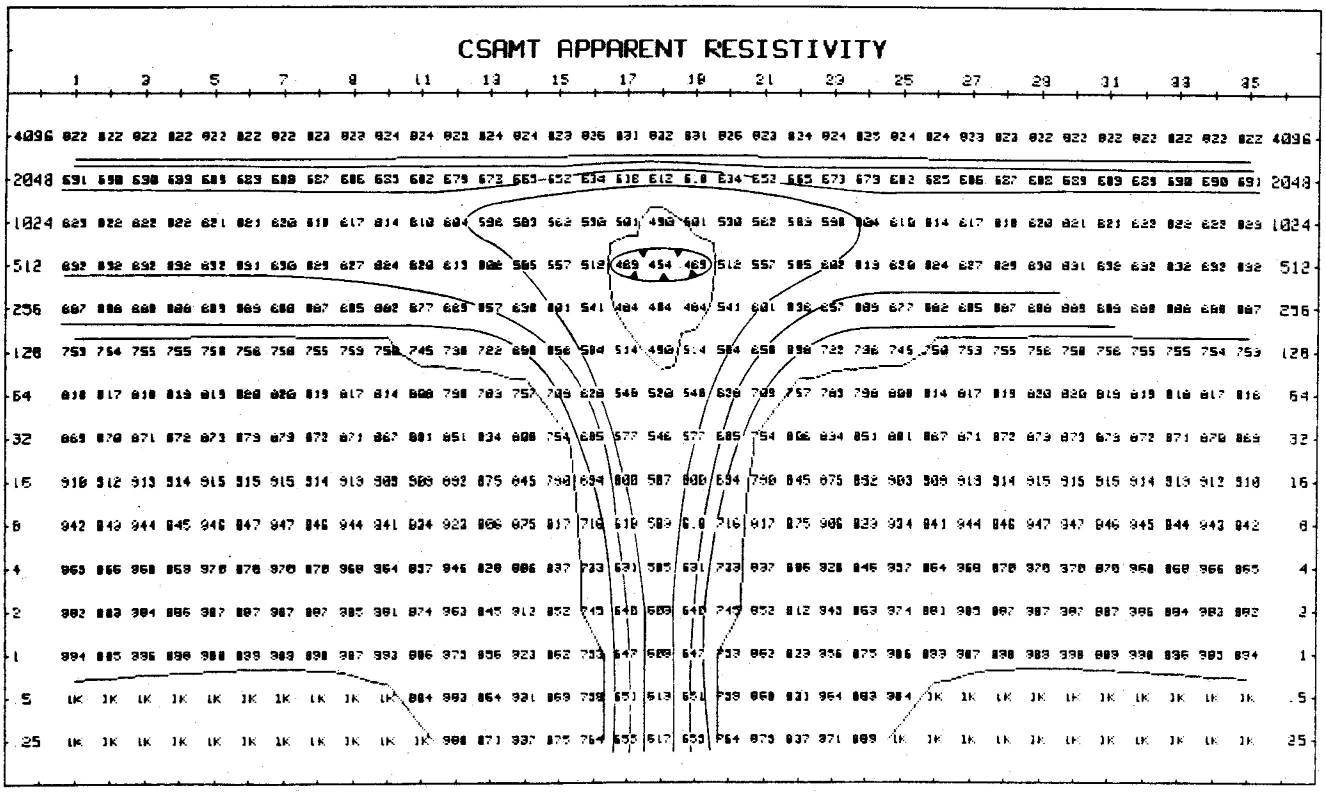

FIGURE 9d

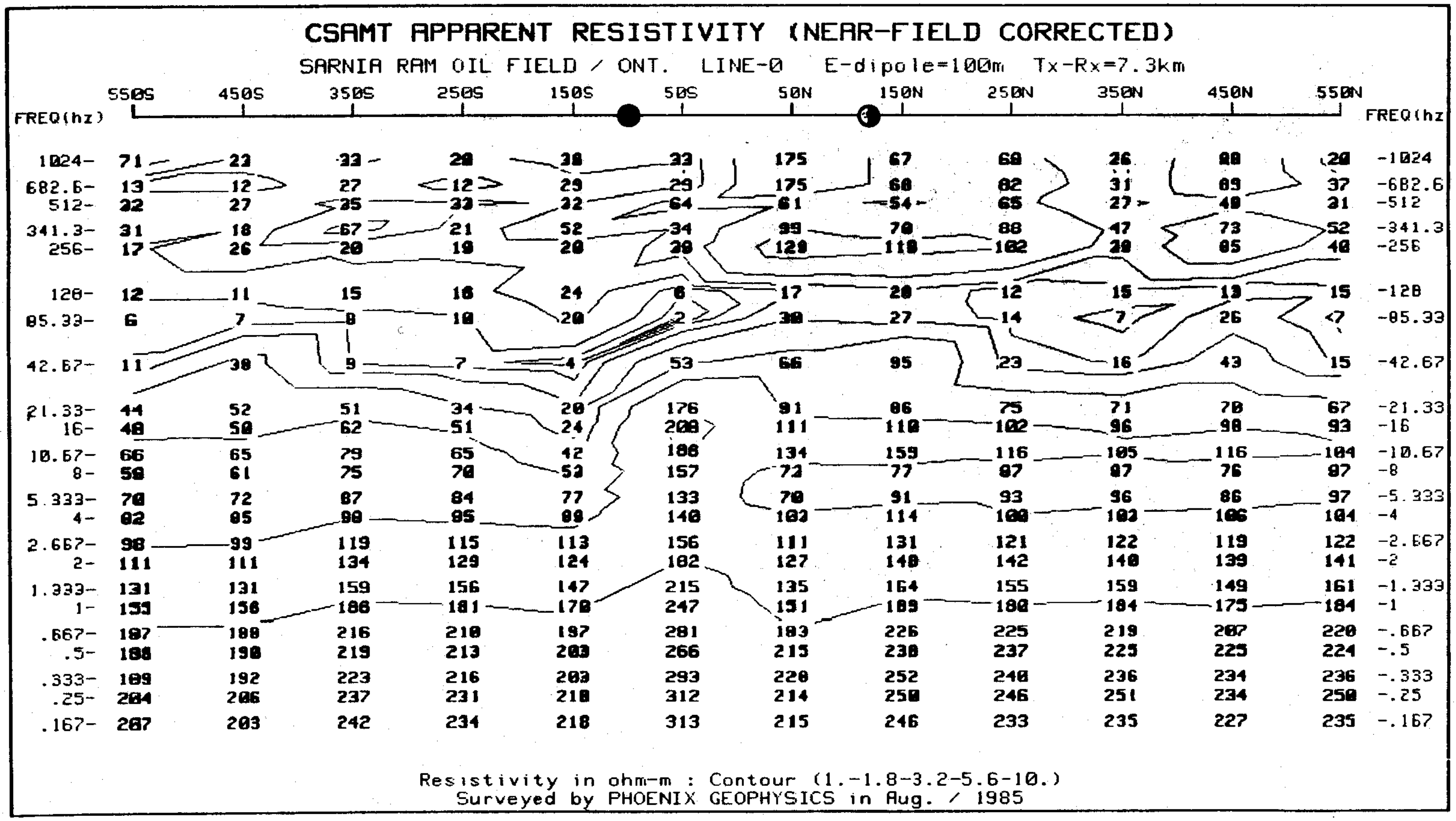
CSAMT APPARENT RESISTIVITY (NEAR-FIELD CORRECTED)
SARNIA RAM OIL FIELD / ONT. LINE-0 E-dipole=100m Tx-Rx=7.3km
550S 450S 350S 250S 150S 50S 50N 150N 250N 350N 450N 550N
FREQ(hz)
FREQ(hz
Resistivity in ohm-m : Contour (1.-1.8-3.2-5.6-10.)
Surveyed by PHOENIX GEOPHYSICS in Aug. / 1985

FIGURE 10b

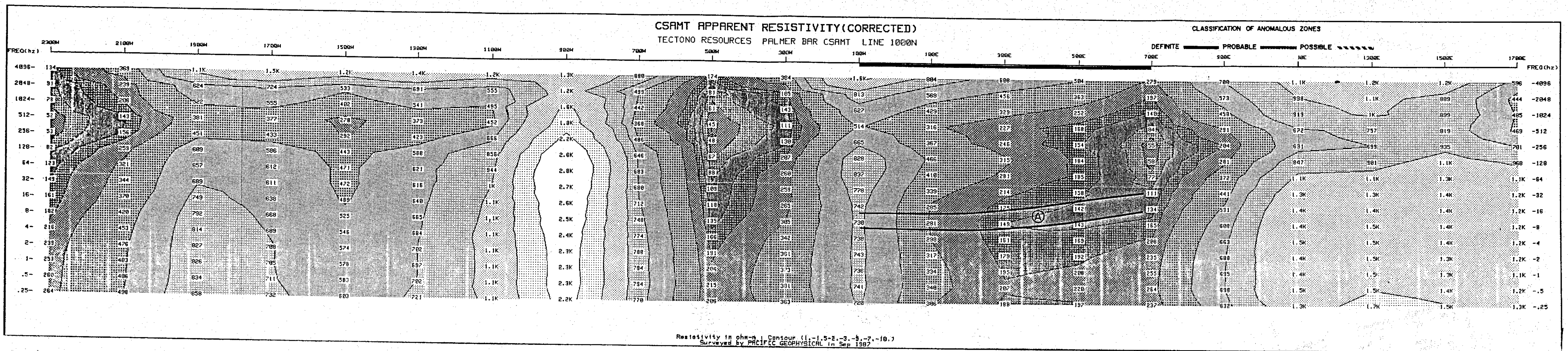

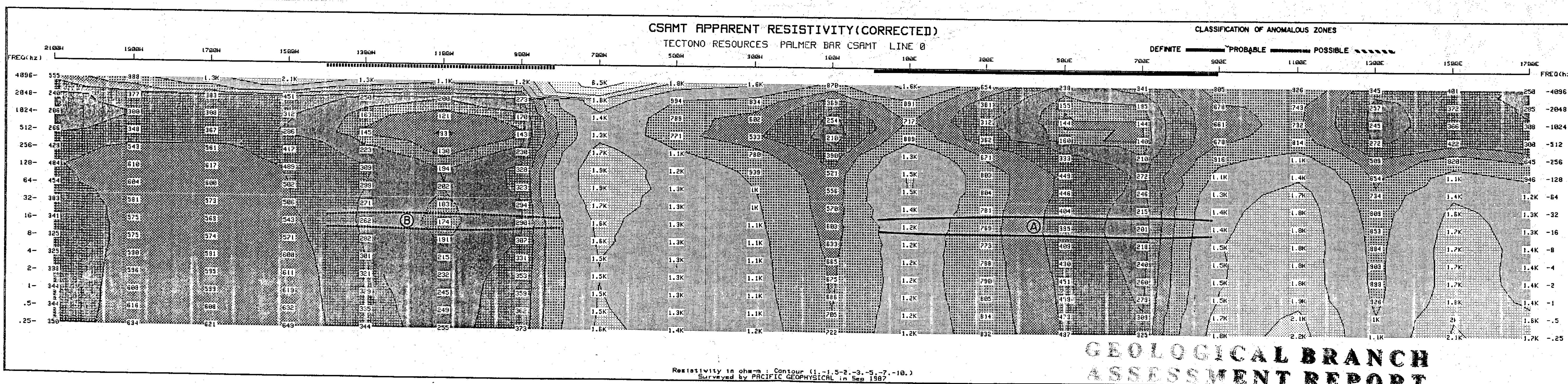

Dwg. No. AMT 5887-1

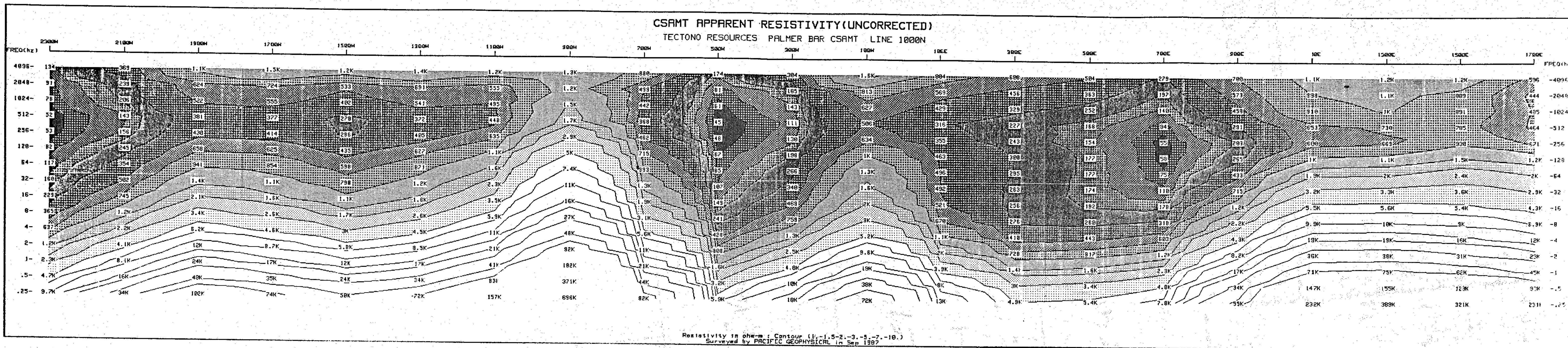

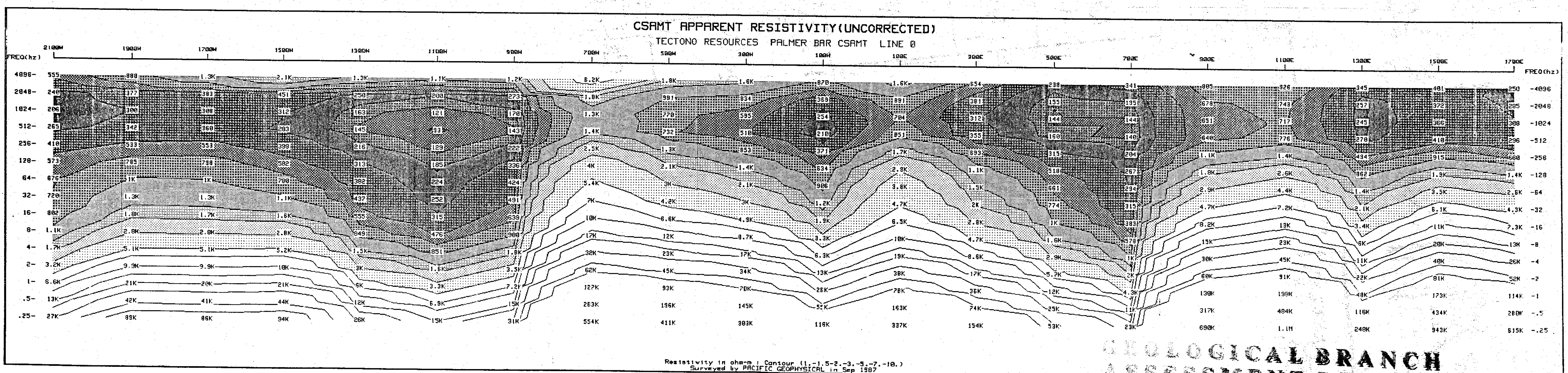

Dwg. No. AMT 5887-2

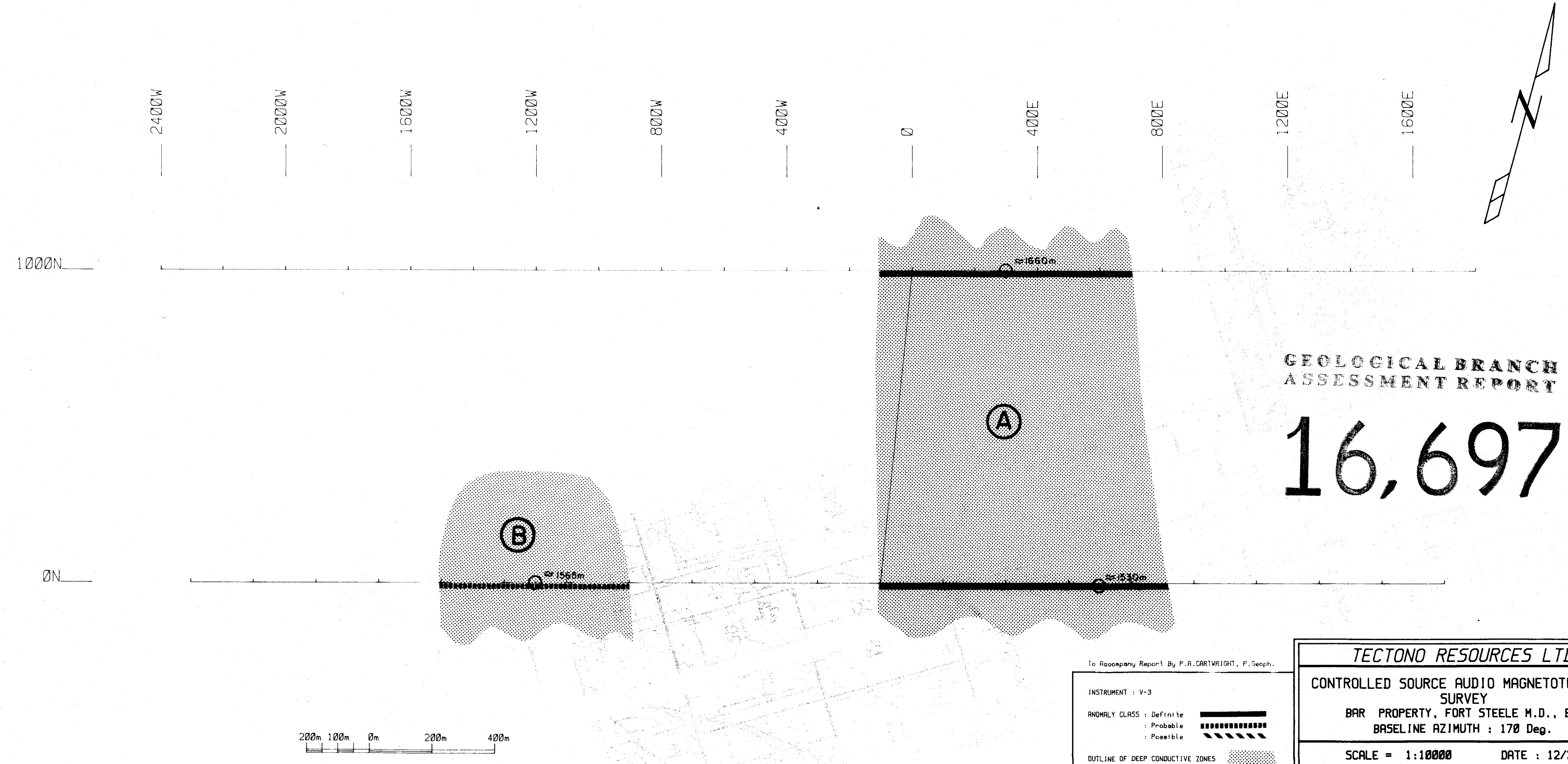

GEOLOGICAL BRANCH
ASSESSMENT REPORT

16,697

To Accompany Report By P.A.CARTWRIGHT, P.Geoph.

INSTRUMENT : V-3

ANOMALY CLASS : Definite
: Probable
: Possible

OUTLINE OF DEEP CONDUCTIVE ZONES

1D INVERSION ○≈ ESTIMATED DEPTH TO DEEP CONDUCTIVE ZONE

TECTONO RESOURCES LTD.

CONTROLLED SOURCE AUDIO MAGNETOTELLURIC SURVEY
BAR PROPERTY, FORT STEELE M.D., B.C.
BASELINE AZIMUTH : 170 Deg.

SCALE = 1:10000 DATE : 12/24/87
SURVEY BY :PAC,RB,BAC NTS : 82G/5
FILE : MTEC Dwg.No.: AMT-2020
Pacific Geophysical Ltd.

Vers. 4.00 Tue 1 Jan 1980 at 1:05 Centre of plot at 300.0W/1200.0N Serial # M87223 Registered User : Pacific Geophysical Ltd.